Improving remote estimation of winter crops gross ecosystem production by inclusion of leaf area index in a spectral model

Radosław Juszczak[1], Bogna Uździcka[1], Marcin Stróżecki[1] and Karolina Sakowska[2]

[1] Meteorology Department, Poznan University of Life Sciences, Poznań, Poland
[2] Institute of Ecology, University of Innsbruck, Innsbruck, Austria

ABSTRACT

The hysteresis of the seasonal relationships between vegetation indices (*VIs*) and gross ecosystem production (*GEP*) results in differences between these relationships during vegetative and reproductive phases of plant development cycle and may limit their applicability for estimation of croplands productivity over the entire season. To mitigate this problem and to increase the accuracy of remote sensing-based models for *GEP* estimation we developed a simple empirical model where greenness-related *VIs* are multiplied by the leaf area index (*LAI*). The product of this multiplication has the same seasonality as *GEP*, and specifically for vegetative periods of winter crops, it allowed the accuracy of *GEP* estimations to increase and resulted in a significant reduction of the hysteresis of *VIs* vs. *GEP*. Our objective was to test the multiyear relationships between *VIs* and daily *GEP* in order to develop more general models maintaining reliable performance when applied to years characterized by different climatic conditions. The general model parametrized with *NDVI* and *LAI* product allowed to estimate daily *GEP* of winter and spring crops with an error smaller than 14%, and the rate of GEP over- (for spring barley) or underestimation (for winter crops and potato) was smaller than 25%. The proposed approach may increase the accuracy of crop productivity estimation when greenness *VIs* are saturating early in the growing season.

Subjects Agricultural Science, Spatial and Geographic Information Science
Keywords LAI, Spectral vegetation indices, NDVI, SAVI, WDRVI, Gross Ecosystem Production, Croplands, Carbon dioxide fluxes

Submitted 15 June 2018
Accepted 21 August 2018
Published 21 September 2018

Corresponding author
Radosław Juszczak,
radoslaw.juszczak@up.poznan.pl

Academic editor
Zhe Zhu

Additional Information and Declarations can be found on page 23

DOI **10.7717/peerj.5613**

INTRODUCTION

Leaf area index (*LAI*) as well as parameters describing carbon dioxide (CO_2) exchange between plants and the atmosphere such as net ecosystem production (*NEP*) and gross ecosystem production (*GEP*) are key biophysical parameters, which are commonly applied to qualitatively and quantitatively characterize the status of vegetation canopies. Numerous studies have confirmed that based on *LAI* the intensity of photosynthesis, transpiration, and productivity of plants might be assessed (*Borge & Leblanc, 2001*; *Breda, 2003*; *Zarco-Tejada, Ustin & Whiting, 2005*). Hence, *LAI* can be used as a proxy of plant growth, biomass and yield, as well as carbon dioxide fluxes exchanged between the ecosystem

and the atmosphere (*Breda, 2003*; *Glenn et al., 2008*). *GEP* reflects the total amount of CO_2 assimilated by plants in photosynthesis (*Waring, Landsberg & Williams, 1998*). It depends on the amount, type and physiological condition of plants, but also on climate and habitat conditions (*Baldocchi et al., 2001*; *Keyser et al., 2000*). *GEP* flux analysis is of importance of studies concerning carbon assimilation efficiency at leaf, plant and ecosystem levels. However, due to the limitations of measurement methods, *GEP* cannot be directly measured *in situ*. State-of-the-art eddy covariance (EC) systems installed on flux towers make it possible to measure only the net fluxes of CO_2 (*NEP*) (*Urbaniak et al., 2016*). *NEP* is defined as a balance of the processes of CO_2 exchange between the ecosystem and the atmosphere and is expressed as a difference between *GEP* and the total amount of CO_2 released by the ecosystem to the atmosphere (ecosystem respiration, R_{eco}) (*Law et al., 2002*).

Remote sensing studies of global vegetation phenology started in 1979 when the meteorological satellite data of Advanced Very High Resolution Radiometer (AVHRR) became available (*Goward & Huemmrich, 1992*). Since then, the following satellite missions (MODIS, LANDSAT, Sentinel-2) have been providing data which allow remote sensing-based estimation of *LAI*, fraction of PAR absorbed by plants (*fAPAR*) and *GEP* of biomes and ecosystems across the globe with higher spatial and temporal resolutions as well as higher accuracy (e.g., *Running et al., 2004*; *Gao et al., 2017*). Traditionally, *GEP* is estimated as a function of vegetation indices (*VI*) related to canopy greenness or based on models including in their formulation also Light Use Efficiency (*LUE*) and/or Photosynthetic Active Radiation (PAR) terms (e.g., *Gitelson et al., 2012*; *Rossini et al., 2012*; *Sakowska et al., 2014*). Many studies have highlighted that simple greenness-related *VIs* can be successfully used for remote sensing-based estimation of *LAI* (e.g., *Gitelson et al., 2003*), chlorophyll content (e.g., *Gitelson et al., 2005*), *fAPAR* (*Sims et al., 2006*), fractional vegetation cover (e.g., *Glenn et al., 2008*) and *GEP* (e.g., *Prince & Goward, 1995*). Among these greenness indices, Normalized Difference Vegetation Index (*NDVI*) has been the most commonly applied, even though it tends to saturate under conditions of moderate- to high aboveground biomass (e.g., *Gitelson, 2004*). For this reason, a big effort was undertaken to develop new *NDVI*-type indices that would not only minimize the soil background influences (e.g., Soil Adjusted Vegetation Index, *SAVI*, *Huete, 1988*), but would also overcome the saturation problem in biophysical parameters estimation (*Gitelson, 2004*). According to existing studies, Modified Simple Ratio (*MSR*, *Chen & Cihlar, 1996*), Renormalized Difference Vegetation Index (*RDVI*, *Roujean & Breon, 1995*), Wide Dynamic Range Vegetation Index (*WDRVI*, *Gitelson, 2004*) or Enhanced Vegetation Index (EVI *Huete et al., 2002*; *Rahman et al., 2005*) are more linearly related to *fAPAR, LAI,* or *GEP* and they allow to estimate these biophysical parameters with higher accuracy. Due to the limited sensitivity of "greenness" indices to a short-term stress which may not impact the chlorophyll content, the Photochemical Reflectance Index (*PRI*) was introduced (*Gamon, Penuelas & Field, 1992*). *PRI* may be an indicator of the *LUE* in the process of photosynthesis (*Gamon, Penuelas & Field, 1992*; *Goerner et al., 2011*; *Penuelas, Filella & Gamon, 1995*) and has been used in *GEP* and *LUE* estimations at leaf, plant and ecosystem levels (e.g., *Rossini et al., 2012*; *Cheng et al., 2014*; *Gitelson, Gamon & Solovchenko, 2017*).

Both the seasonal dynamics and relationships between *VIs* and biophysical parameters have been analyzed in numerous studies. The relationships of spectral data have been investigated in relation to *LAI* (*Baret & Guyot, 1991*; *Law & Waring, 1994*; *Spanner et al., 1990*; *Zheng & Moskal, 2009*), *fAPAR* (*Asrar et al., 1984*; *Wang et al., 2004*; *Sakowska, Juszczak & Gianelle, 2016*), and the CO_2 fluxes exchanged between the ecosystem and the atmosphere – particularly *GEP* (*Rossini et al., 2012*; *Sakowska et al., 2014*; *Skinner, Wylie & Gilmanov, 2011*; *Uździcka et al., 2017*), *NEP* (*Hassan, Bourque & Meng, 2006*; *Propastin & Kappas, 2009*; *Veroustraete, Patyn & Myneni, 1996*) and *NPP* (*Gower, Kucharik & Norman, 1999*; *Hunt, 1994*; *Paruelo et al., 1997*; *Ruimy, Saugier & Dedieu, 1994*). These kind of relationships were mostly analyzed for individual ecosystems (e.g., grasslands - *Rossini et al., 2012*; *Sakowska et al., 2014*, peatlands - *Chojnicki, 2013*, savanna - *Sjöström et al., 2009*, forests - *Xiao et al., 2004*), or crop species on a separate basis (e.g., maize - *Gitelson et al., 2003*; *Gitelson et al., 2014*; *Peng et al., 2011*, maize and soybean - *Gitelson et al., 2012*, rice - *Inoue et al., 2008*, wheat - *Wu et al., 2009*).

In this paper we investigated the relationships between *LAI, VIs* and daily values of *GEP* determined using chamber measurements conducted on four crops grown in Poland. Similar kind of analyzes where *GEP* was correlated with *VIs*, *LAI* or chlorophyll content, and/or products of *VIs* and PAR have been presented in many studies (e.g., *Rossini et al., 2012*; *Rossini et al., 2014*; *Sakowska et al., 2014*; *Gitelson et al., 2012*; *Gitelson et al., 2014*). The relationships were investigated with an average midday *GEP* (e.g., *Gitelson et al., 2006*; *Rossini et al., 2012*; *Sakowska et al., 2014*) or with a daily sum of *GEP* (e.g., *Rossini et al., 2012*; *Gitelson et al., 2014*), but in all of these studies *GEP* was determined based on the ecosystem-scale EC measurements. In this study, *GEP* was obtained based on plot-scale chamber measurements. Although these measurements have some limitations (e.g., *Urbaniak et al., 2016*), the biggest advantage of chamber systems is that both *NEP* and *Reco* fluxes are measured directly and subsequently which facilitates the calculation of *GEP*.

In order to obtain remote sensing-based model which allows to estimate daily *GEP* of crops independently from the type of the crop and climatic conditions with reliable performance, we studied a 3-year dataset (2011–2013) consisting of spectral and biophysical data for two winter (wheat and rye) and two spring (barley, potato) crops. Our specific objectives were to test (1) the accuracy of daily *GEP* estimations with remote sensing-based models fed with different *VIs* and *VIs*PAR* and a model based on *LAI*, and (2) whether the accuracy of *GEP* estimations increases when products of *VI* and *LAI* are included in the model. Besides, considering that for some crops the hysteresis of the relationships between *VIs* and biophysical parameters is observed (*Peng et al., 2017*), we aimed at developing a simple linear empirical model based on *VIs* and *LAI* in order to reduce hysteresis of the *VIs vs. GEP* relationships between vegetative and reproductive phases of crop development cycle and to increase the accuracy of daily *GEP* (GEP_d) estimations of croplands. According to our knowledge this is also the first study in which CO_2 fluxes measured with chambers are combined with both *LAI* and *VIs*.

MATERIAL AND METHODS

Experimental site

Measurements were conducted at the Brody Experimental Station (52°26′N, 16°18′E) on plots of the long-term experiment that has been conducted since 1957 by the Department of Agronomy, Poznań University of Life Sciences, Poland (*Blecharczyk et al., 2016*). Crops were grown in the crop rotation and monoculture systems under 11 different fertilization regimes (no fertilization, manure, manure + NPK, NPK + Ca-CaO, NPK, NP, NK, PK, N, P, K). The measurements presented in this paper were performed on four crop species: potato (var. *Wineta*), spring barley (var. *Nadek*), winter wheat (var. *Turkis)* and winter rye (var. *Dankowskie Zlote)*, grown in a seven-year rotation (potato → spring barley → winter triticale →1- and 2-year alfalfa → winter wheat → winter rye). The investigated crops were fertilized with NPK (90 kg N ha^{-1} a^{-1}, 60 kg P_2O_5 ha^{-1} a^{-1}, 120 kg K_2O ha^{-1} a^{-1}) with an addition of Ca-CaO (1.5 Mg CaO ha^{-1} a^{-1}) and grown in 6 × 11 m plots separated by 0.5 m wide bare soil stripe. The annual mean air temperature of the study area is 7.9 °C, while the annual precipitation sum is 571 mm (average for 1959–1999). The soils are classified as *Albic Luvisols* developed on loamy sands overlying loamy material (*Majchrzak et al., 2016*).

Chamber CO_2 fluxes and flux modelling

Measurements of CO_2 fluxes (*NEP*, R_{eco}) were taken using a closed dynamic portable chamber system, which consisted of a transparent and non-transparent chambers to measure *NEP* and R_{eco} fluxes, respectively (*Chojnicki et al., 2010*; *Juszczak et al., 2013*). Measurements were made in two subplots for each crop. The transparent chamber was made of three mm-thick Plexiglas (Evonik Industries, Darmstadt, Germany), as this material has a high solar radiation transmittance (approximately 90%, *Acosta et al., 2017*; *Hoffman et al., 2015*). The non-transparent chamber was made of three mm-thick white PVC to ensure dark conditions inside the chamber. The chambers had dimensions of 0.78 × 0.78 × 0.50 m and a total volume of 0.296 m^3. In case of winter rye and winter wheat, the extensions of 0.5 m height were used (made of the same material) in order to adopt the height of chamber to the height of the canopy. During the measurements, chambers were placed on square PVC collars (0.75 × 0.75 m), inserted into the soil just after sowing. The insertion depth of the collars was 15 cm. The chambers were equipped with a set of computer fans (1.4 W; 1,500 rpm each) mixing the air and a vent to equilibrate pressure in the chamber headspace. The air temperature inside the chamber headspace was measured with a radiation-shielded thermistor (T-107; Campbell Scientific, Logan, UT, USA) at a height of 0.3 m, or 0.8 m for short and tall chambers, respectively (*Juszczak, Acosta & Olejnik, 2012*; *Juszczak et al., 2013*). The CO_2 concentration changes in the chamber was measured using LI-820 gas analyzer (LI-COR Inc., Lincoln, NE, USA). The air was circulated between the chamber and the analyzer in a closed loop with the flow rate of 0.7 l min^{-1}. In order to keep the air temperature inside the chamber headspace stable, the transparent chamber was cooled with a passive system described in *Acosta et al. (2017)*.

Chamber measurements were taken every 3–5 weeks throughout the entire year (including winter) on cloudless days from sunrise to late afternoon (*Uździcka et al., 2017*). However, when any clouds appeared (usually in the afternoon) a particular attention was paid to perform measurements at stable PAR conditions. Overall, 37 chamber campaigns were conducted in the years 2011–2013. Measurements of *NEP* and R_{eco} were taken on each of the soil frames several times per day (from five to 12, depending on the daytime length). A single *NEP* measurement took 120 seconds, and the subsequent *NEP* measurement at the same plot was taken before the value of incoming *PAR* changed by more than 150 μmol m^{-2} s^{-1}. A single measurement of R_{eco} took 180 seconds and the succeeding measurements were taken before the soil temperature at the same plot changed by more than 0.5 °C. The CO_2 flux (F) in μmols m^{-2} per time unit (t) was calculated from the gas concentration change in the chamber headspace ($\frac{\Delta C}{\Delta t}$), the chamber volume ($V$) and the enclosed soil area (A) from the following equation (*Urbaniak et al., 2016*):

$$F = \frac{\Delta C}{\Delta t} \cdot \frac{V}{A \cdot M_v} \quad (1)$$

where M_v (m^3 mol^{-1}) is the molar volume of air at a given chamber air temperature and pressure. The determination coefficient (r^2) was calculated for each single chamber closure time and if $r^2 < 0.8$, the fluxes were excluded from the analyzes. To ensure that good quality near-zero fluxes were not erroneously excluded by this criteria, all rejected fluxes were visually inspected.

Fluxes of *NEP*, R_{eco} and *GEP* for measurement days and periods between campaigns were calculated using a simple empirical model described by *Drösler (2005)* and farther elaborated by *Hoffman et al. (2015)*. For this purpose, for each day of measurements, the relationships between measured R_{eco} and temperature were established by fitting to the campaign-specific flux dataset the temperature dependent Arrhenius-type respiration model of *Lloyd & Taylor (1994)*. Using the parameters of this model, R_{eco} values at the time of the *NEP* measurements were estimated based on the measured temperatures (*Juszczak et al., 2013*). In the next step, based on such estimated R_{eco} and measured *NEP*, *GEP* was calculated according to the formula $GEP = NEP + R_{eco}$. Subsequently, the calculated *GEP* fluxes were correlated with measured *PAR*, fitting to the campaign-specific *GEP* dataset a rectangular hyperbolic light response Michaelis–Menten kinetic model (*Michaelis & Menten, 1913*). The R_{eco} and *GEP* model parameters were interpolated linearly for the periods between the campaigns with a 30-minute step, so that, based on the continuous time series of measured *PAR* and temperature (means for 30-minute periods), *GEP* and R_{eco} was calculated. *NEP* was calculated from the formula $NEP = GEP - R_{eco}$. Daily sums of *GEP* (so called daily *GEP* (GEP_d)) were calculated as a sum of all 30-minute *GEP* fluxes estimated for each day with the flux model in between sunrise to sunset.

Measurements of *LAI* and spectral characteristics of the crops

LAI and multispectral data were collected during the growing season, from March to October, at one- to two-week intervals. At the spring barley plots measurements started in the middle of April (after sowing), whereas in case of potatoes in the 2nd week of May

Table 1 Spectral vegetation indices calculated from ground-based spectroscopy and presented in this study.

Spectral vegetation index	Formulation	Reference
NDVI	$NDVI = \frac{\rho 850 - \rho 670}{\rho 850 + \rho 670}$	*Rouse et al. (1973)*
SAVI	$SAVI = \frac{\rho 850 - \rho 670}{\rho 850 + \rho 670 + L}(1 + L)$	*Huete (1988)*
PRI	$PRI = \frac{\rho 570 - \rho 531}{\rho 570 + \rho 531}$	*Gamon, Penuelas & Field (1992)*
WDRVI	$WDRVI = \frac{\alpha * \rho 850 - \rho 670}{\alpha * \rho 850 - \rho 670}$	*Gitelson (2004)*

Notes.

ρ, reflectance at a given wavelength; NDVI, Normalized Difference Vegetation Index; SAVI, Soil Adjusted Vegetation Index; PRI, Photochemical Reflectance Index; WDRVI, Wide Dynamic Range Vegetation Index.

(after planting). Only the data collected in the period between April and the 2nd week of August (just after harvesting) was considered in the analyzes, hence we did not present nor analyzed data collected after sowing of winter crops and after harvest. The dates of the measurement campaigns were selected so that these measurements could overlap with chamber measurements of CO_2 exchange. However, when the weather conditions were not stable due to appearing clouds, the measurements were repeated on the first sunny day following the chamber measurements. 36 measurement campaigns were organized in the 3-year period (2011–2013). Spectral measurements were carried out only on sunny days, always around the solar noon (between 10:00–14:00). Measurements of *LAI* and reflectance were taken at each plot in three replications, always in the same locations.

LAI was measured by means of the SunScan system (Delta-T Devices, Cambridge, UK). The spectral characteristics of the surface of plant-covered plots were measured using two 4-channel SKR1850 sensors (SKYE Instruments Ltd., Llandrindod Wells, UK) mounted on a portable SKL908 device (Spectrosense2+). Incident and reflected radiation was recorded at central wavelengths of 531, 570, 670 and 850 nm with 10 nm bandwidths. Next, applying the methodology developed by SKYE instruments Ltd. (SpectroSense2+ Manual), vegetation indices (*NDVI, SAVI* and *PRI*) were calculated (Table 1) according to the formula:

$$VI = \frac{(Z \cdot R1_r \cdot Y) - (R2_r \cdot X)}{(Z \cdot R1_r \cdot Y) + (R2_r \cdot X)}$$

where *VI* is a vegetation index, *Z* is a ratio sensitivity of reflected $R1_r$:$R2_r$; *X* and *Y* are incident readings for $R1_i$ and $R2_i$, respectively (in μmol $m^{-2}s^{-1}$), while $R1_r$ and $R2_r$ correspond to reflected signal readings for wavelengths *R1* and *R2* (in nanoamps). For *NDVI* and *SAVI*, *R1* and *R2* correspond to 850 nm and 670 nm wavelengths respectively, while for *PRI* they correspond to wavelengths 570 nm and 531 nm. To calculate *SAVI*, the above formula was modified according to equation provided in Table 1. Wide Dynamic Range Vegetation Index was calculated from *NDVI* from the equation: $WDRVI = [(\alpha + 1)$ NDVI $+ (\alpha - 1)]/[(\alpha - 1)$NDVI $+ (\alpha + 1)]$, where $\alpha = 0.2$ (*Vina & Gitelson, 2005*). In order to express values of this *VI* in positive numbers, sWDRVI was calculated from equation ($sWDRVI = (WDRVI + 1)/2$).

Table 2 The models tested for GEP_d estimation in the present study.

Model	Model formulation
1	$GEP_d = a \cdot LAI + b$
2	$GEP_d = a \cdot VI + b$
3	$GEP_d = a \cdot (VI \cdot PAR_d) + b$
4	$GEP_d = a \cdot (VI \cdot LAI) + b$

Models for GEP estimations

Daily *GEP* (GEP_d) were estimated based on linear regressions assuming a direct linear relationship between GEP_d and *LAI* (model 1), GEP_d and *VIs* (model 2), GEP_d and a product of *VIs* and mean daily *PAR* calculated for the time between the sunrise and sunset $-PAR_d$ (model 3), as well as GEP_d and a product of *VIs* and *LAI* (model 4) (Table 2). All the models were tested based on the combined multi-year (2011–2013) dataset for each crop species separately, as well as for all cereals: winter wheat, winter rye and spring barley (i) and cereals and potatoes (ii) considered together in order to develop the general models for GEP_d estimations for croplands. The general models with the best goodness of fit were then tested for each crop independently.

Statistical analysis

Pearson's correlation analysis was used to test the significance of the relationships between GEP_d and (i) *LAI*; (ii) *VIs* (*NDVI*, *SAVI*, *WDRVI*, *PRI*); (iii) *VIs*PAR*$_d$; and (iv) *VIs* LAI*. Analyzes were conducted for each crop independently and for the combined datasets of cereals, as well as for cereals and potatoes considered together.

Each of the four analyzed models' coefficients were found by fitting each model against GEP_d. Goodness of fit statistics (coefficient of determination, R^2; root means square error, *RMSE* in gCO_2-C $m^{-2}d^{-1}$; and normalized root mean square error, *NRMSE* in %) were computed to compare the performance of the models.

In order to determine if there are significant differences in relationships between GEP_d and *VIs* between the vegetative and reproductive phases of crop development, the two-sample *t*-test approach was applied. The differences between analyzed relationships were considered to be significant if *p*-value obtained from the test was lower than 0.05.

Due to limited number of data (*n* equals from 21 to 26, depending on the crop and *VI*), validation of the best performing general models developed based on the combined dataset for cereals and potatoes was conducted for each crop species separately by comparing GEP_d retrieved from chamber CO_2 fluxes with GEP_d estimated based on the spectral model individually for each crop.

RESULTS

The seasonal variations of meteorological conditions for the analyzed growing seasons are presented in Fig. 1. The seasonal mean air temperatures were 14.0 °C, 13.9 °C and 12.4 °C, while the sums of precipitation were 331 mm, 363 mm and 344 mm for the periods between 1st of March and 31st of August of 2011, 2012 and 2013, respectively. The

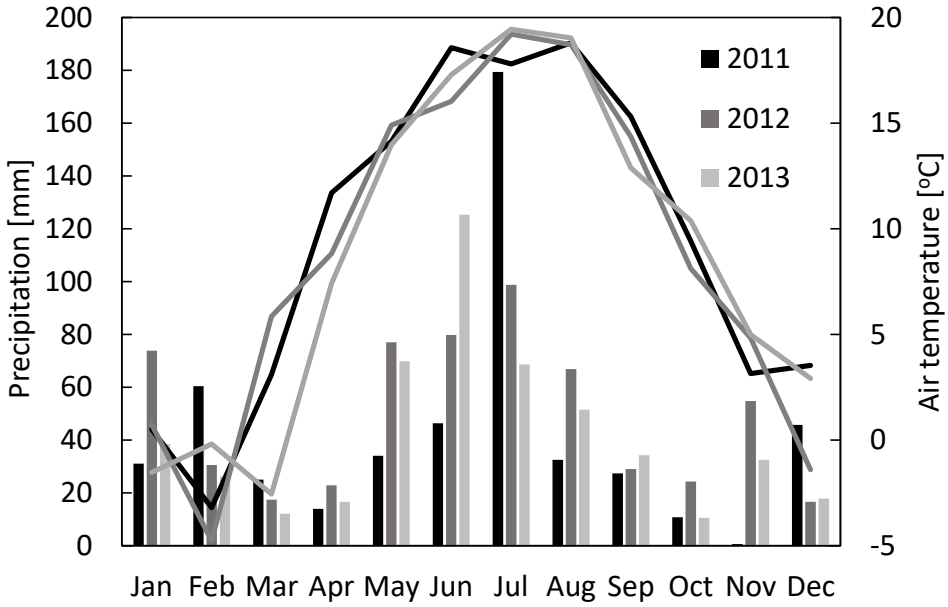

Figure 1 **Monthly sums of precipitation and mean air temperatures in Brody for 2011–2013.**
Full-size DOI: 10.7717/peerj.5613/fig-1

highest amount of precipitation was recorded in July 2011 (179 mm), July 2012 (99 mm), and June 2013 (125 mm). It has to be highlighted that sums of precipitation in May and June of 2011 - the two most critical for the plant growth months - were nearly two-times smaller than during the same period of the two following years. Considering the long term climatological records for this region, 2011 and 2013 are considered as warm (with the mean annual temperatures of 9.4 °C and 8.7 °C, respectively) and dry years (507 mm and 503 mm, respectively), while 2012 was considered as a warm (with the mean annual temperature of 9.0 °C) and wet (592 mm) year (*Uździcka et al., 2017*). During the growing period of the main crop (March-August) the average PAR_d was 659 (±241), 664 (±224) and 641 (±223) μmol $m^{-2}s^{-1}$ in 2011, 2012 and 2013, respectively, with the maximum values of 1,011–1,068 μmol $m^{-2}s^{-1}$ (Fig. 2A).

The seasonal variations of *LAI* and GEP_d for all analyzed years and crops are presented in Fig. 2. The maximum *LAI* (LAI_{max}) and GEP_d of winter crops were recorded in the first week of May in 2011 and the last week of May-beginning of June in 2012 and 2013. In case of spring barley the *LAI* and GEP_d peaks occurred during the last week of May in 2011 and 2012 and in mid-June in 2013. Maximum rates of GEP_d and *LAI* at potato plots were recorded in the 2nd week of June in 2013 and 3rd week of June in 2011 and 2012. Maximum values of GEP_d and *LAI* for winter wheat were observed nearly at the same time, with just a 2-week shift in 2011. The LAI_{max} was 2.7, 3.3, and 4.4 m^2m^{-2} for winter wheat; 2.9, 5.0, and 4.3 m^2m^{-2} for winter rye; 2.5, 4.0 and 4.0 m^2m^{-2} for spring barley and 1.8, 3.4 and 3.2 m^2m^{-2} for potato, in 2011, 2012 and 2013, respectively (Table 3). The comparison of LAI_{max} between the investigated years showed that for all the investigated crops LAI_{max} was lower in 2011 than in both 2012 and 2013. There were no differences in

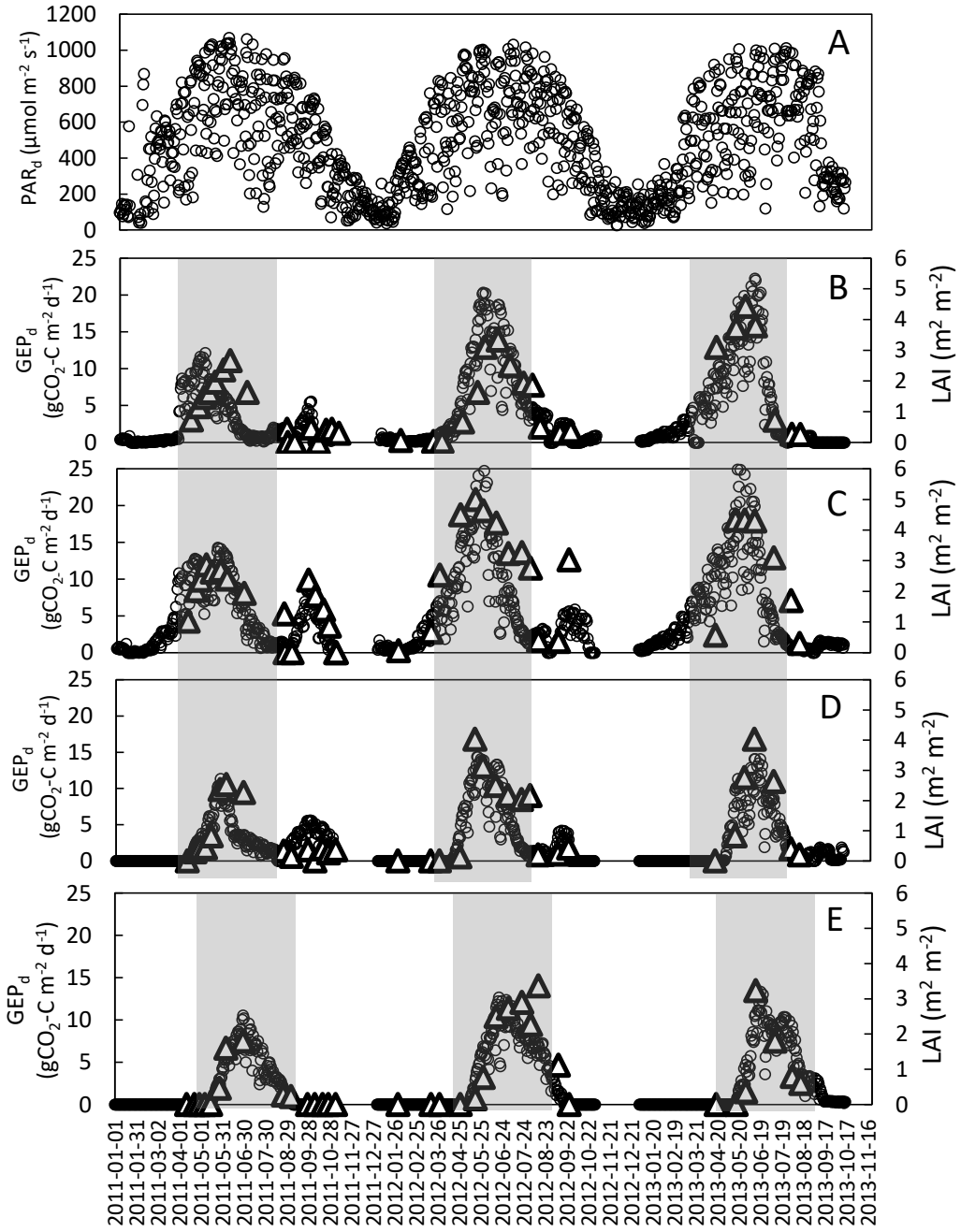

Figure 2 Seasonal variations of mean daily PAR (PAR_d) at the study site and daily *GEP* (GEP_d; circles) and *LAI* (triangles) for the analyzed crops in the years 2011–2013. (A) mean daily PAR; (B) refers to winter wheat; (C) winter rye; (D) spring barley and (E) potatoes. Shaded areas indicate periods when the main crop was present in the field (these periods were analyzed in this study).

Full-size DOI: 10.7717/peerj.5613/fig-2

Table 3 Seasonal mean and maximum values of GEP_d, *NDVI*, *SAVI*, *sWDRVI*, *PRI*), canopy height (H_{canopy}) and fractional cover (*F*%) for the analyzed crops in the growing periods of 2011, 2012 and 2013.

		Units	Winter wheat		Winter rye		Spring barley		Potatoes	
			mean	max.	mean	max.	mean	max.	mean	max.
2011	GEP_d	gCO_2-Cm^{-2} s^{-1}	3.60(±3.4)	12.14	6.31(±4.3)	14.30	3.75(±2.7)	11.33	2.77(±3.1)	10.54
	LAI	m^2 m^{-2}	1.56(±0.7)	2.67	2.14(±0.6)	2.87	1.19(±1.0)	2.53	0.83(±0.8)	1.80
	H_{canopy}	m	0.41(±0.2)	0.78	0.78(±0.6)	1.50	0.22(±0.2)	0.62	0.15(±0.2)	0.55
	F%	%	0.38(±0.2)	0.60	0.66(±0.2)	0.90	0.37(±0.3)	0.85	0.19(±0.3)	0.70
	NDVI	–	0.65(±0.2)	0.79	0.68(±0.2)	0.88	0.51(±0.3)	0.85	0.23(±0.3)	0.77
	SAVI	–	0.17(±0.1)	0.28	0.18(±0.1)	0.33	0.16(±0.1)	0.30	0.08(±0.1)	0.28
	sWDRVI	–	0.47(±0.2)	0.63	0.55(±0.2)	0.75	0.37(±0.2)	0.71	0.37(±0.2)	0.61
	PRI	–	−0.19(±0.02)	−0.18	−0.18(±0.02)	−0.15	−0.20(±0.02)	−0.17	−0.19(±0.01)	−0.18
2012	GEP_d	gCO_2-Cm^{-2} s^{-1}	7.24(±5.9)	20.33	8.78(±7.2)	31.65	5.78(±4.5)	14.36	6.31(±3.2)	12.66
	LAI	m^2 m^{-2}	1.73(±1.15)	3.33	3.12(±1.6)	5.00	2.05(±1.3)	4.03	1.84(±1.3)	3.37
	H_{canopy}	m	0.54(±0.4)	0.99	0.95(±0.6)	1.59	0.34(±0.3)	0.66	0.30(±0.3)	0.72
	F%	%	0.41(±0.3)	0.80	0.75(±0.3)	0.95	0.56(±0.4)	0.95	0.39(±0.4)	0.95
	NDVI	–	0.48(±0.3)	0.84	0.56(±0.3)	0.90	0.44(±0.3)	0.84	0.55(±0.3)	0.88
	SAVI	–	0.15(±0.1)	0.31	0.18(±0.1)	0.31	0.17(±0.2)	0.38	0.22(±0.2)	0.49
	sWDRVI	–	0.39(±0.2)	0.70	0.49(±0.2)	0.79	0.35(±0.2)	0.69	0.46(±0.2)	0.77
	PRI	–	−0.19(±0.01)	−0.17	−0.20(±0.03)	−0.16	−0.22(±0.02)	−0.20	−0.20(±0.02)	−0.23
2013	GEP_d	gCO_2-Cm^{-2} s^{-1}	6.91(±6.3)	22.24	8.13(±6.3)	27.29	5.37(±4.2)	14.06	5.66(±3.6)	13.33
	LAI	m^2 m^{-2}	2.33(±1.8)	4.43	2.66(±1.8)	4.33	1.81(±1.5)	4.02	1.13(±1.2)	3.23
	H_{canopy}	m	0.38(±0.3)	0.82	0.80(±0.6)	1.40	0.28(±0.2)	0.60	0.24(±0.2)	0.45
	F%	%	0.49(±0.4)	0.90	0.62(±0.3)	0.90	0.42(±0.4)	0.90	0.30(±0.2)	0.50
	NDVI	–	0.58(±0.4)	0.88	0.55(±0.3)	0.85	0.57(±0.3)	0.89	0.47(±0.3)	0.70
	SAVI	–	0.25(±0.2)	0.44	0.24(±0.1)	0.38	0.33(±0.1)	0.45	0.22(±0.1)	0.30
	sWDRVI	–	0.58(±0.2)	0.76	0.46(±0.2)	0.72	0.44(±0.2)	0.78	0.38(±0.2)	0.56
	PRI	–	−0.19(±0.03)	−0.17	−0.20(±0.03)	−0.16	−0.17(±0.1)	0.00	−0.20(±0.01)	−0.19

Notes.

For winter crops growing periods started on the 1st of March; for spring barley they started in the middle of April and lasted until skimming in the last week of August; for potato the growing seasons started in the second week of May and ended in the middle of September each year.

LAI_{max} for spring barley and potato in 2012 and 2013, while LAI_{max} was the highest for winter rye in 2012 and for winter wheat in 2013.

Similarly to *LAI*, the maximum daily *GEP* values of all the investigated crops were lower in 2011 compared to 2012 and 2013. The GEP_d of winter crops was 45% (winter rye) to 60% (winter wheat) lower in 2011 than in the two following years. The differences in maximum GEP_d of the spring crops (spring barley and potato) between 2011 and 2012, 2013 were smaller than in case of winter crops (20%). Maximum rates of GEP_d for winter wheat reached 12.1, 20.3 and 22.2 gCO_2-Cm^{-2} d^{-1} and for winter rye 14.3, 31.6 and 27.3 gCO_2-Cm^{-2} d^{-1} in 2011, 2012 and 2013, respectively, while for spring barley and potato GEP_d were 11.3 and 10.5 gCO_2-Cm^{-2} d^{-1} in 2011, 14.4 and 12.3 gCO_2-Cm^{-2} d^{-1} in 2012, and 14.0 and 13.3 gCO_2-Cm^{-2} d^{-1} in 2013, respectively (Table 3).

Maximum values of *NDVI* and *SAVI* were observed nearly at the same time as the peaks of *LAI* and GEP_d (data shown in File S2). Moreover they were also lower in 2011 than in

the other two years, even though the observed differences in maximum *VIs* values were less prominent than the differences in the analyzed biophysical parameters (Table 3). All these data clearly indicate the effect of drought which occurred in the late spring - early summer of 2011, when sums of precipitation were 50% smaller than the precipitation observed in the same period of 2012 and 2013.

The analysis of linear regression revealed that *LAI* explained minimum 60% of the variability in GEP_d (Table 4). *NDVI* and *SAVI* explained from 52% to 72% of the variability in GEP_d for winter crops and up to 81%-91% for spring crops, when crops were considered separately. For crop-combined dataset, which consisted of the data of all the analyzed crops, *NDVI* and *SAVI* explained 50% to 65% of the variability in GEP_d. *SAVI*-based models worked better only in case of models developed for winter rye, while in case of other crops it did not lead to more accurate estimations of GEP_d. Moreover, the *SAVI*-based models ($R^2 = 0.50$, NRMSE = 18.24%) developed for all the crops together were less accurate than *NDVI*-based models ($R^2 = 0.65$, NRMSE = 15.29%). The *sWDRVI,* which was expected to be more linearly correlated with GEP_d, explained between 50% (winter rye) to 86% (spring barley) of the GEP_d variability and did not improve the accuracy of GEP_d estimations in the crop-combined model ($R^2 = 0.65$, NRMSE = 15.60%). The highest accuracy of model 2 was obtained for potato (if based on *NDVI*; $R^2 = 0.91$, NRMSE = 10.94%). Inclusion of PAR_d into model 3 did not improve estimations of GEP_d for any of the investigated crops nor for the crop-combined datasets.

The inclusion of *LAI* into the "*VIs*"-based models resulted in a general increase of their performance in case of the winter crops (Table 4). The highest increase of the accuracy of GEP_d estimations was found for *NDVI*-based models. For winter wheat, RMSE decreased from 4.31 to 3.56 gCO_2-C m^{-2} d^{-1}, while NRMSE decreased from 19.83% to 16.38% after inclusion of *LAI* into *NDVI*-based model. For winter rye, the changes were even more prominent - RMSE decreased from 4.72 to 3.14 gCO_2-C m^{-2} d^{-1}, whereas NRMSE decreased from 20.15% to 13.42%. Inclusion of *LAI* into *NDVI*-based models developed for spring barley and potatoes led to a decrease of the accuracy of GEP_d estimations (Table 4). For spring barley RMSE and NRMSE increased from 1.73 to 1.79 gCO_2-C m^{-2} d^{-1} and from 12.33% to 12.70%, respectively. The highest reduction of the model accuracy was observed for potatoes - RMSE and NRMSE increased from 1.26 to 2.10 gCO_2-C m^{-2} d^{-1} and from 10.94% to 18.30%, respectively.

For more general models developed for the cereals and crop-combined datasets the inclusion of *LAI* into the *VIs*-based models also resulted in an improvement of model performance. RMSE and NRMSE of *NDVI* and *LAI*-based models were the smallest and decreased from 4.09 to 3.42 gCO_2-C m^{-2} d^{-1} and from 17.02% to 14.39% for cereals-combined models, and from 3.67 to 3.26 gCO_2-C m^{-2} d^{-1} and from 15.29% to 13.57% for crop-combined datasets, respectively (Table 4). That is why we used the most general and the best fitting *NDVI*LAI* model developed for all the crops together (cereals & potatoes, Fig. 3) to estimate GEP_d values for each crop separately (Fig. 4). Although there is a good agreement between observed and predicted GEP_d values for all the crops (Fig. 3), GEP_d estimated for winter crops and potatoes was underestimated, while GEP_d of spring barley was overestimated, but the rate of over- or under-estimation did not exceed 25% (Fig. 4).

Table 4 Summary of the statistics of linear regressions between *LAI*, *VIs* and GEP_d for each crop individually, for all cereals (winter and spring crops) and for cereals and potato grouped together.

Model		Winter wheat					Winter rye				
		n	R^2	*RMSE*	*NRMSE*	*p*	*n*	R^2	*RMSE*	*NRMSE*	*p*
		–	–	gCO2-C m^{-2} s^{-1}	%	–		–	gCO2-C m^{-2} s^{-1}	%	–
1	*LAI*	26	0.62	4.07	18.75	<0.0001	26	0.60	4.34	18.54	<0.0001
2	*NDVI*	25	0.56	4.31	19.83	<0.0001	26	0.52	4.72	20.15	<0.0001
	SAVI	21	0.59	3.93	18.56	<0.0001	24	0.72	3.53	15.07	<0.0001
	sWDRVI	25	0.62	4.03	18.54	<0.0001	26	0.50	4.84	20.67	<0.0001
	PRI	22	0.49	4.64	19.79	<0.001	21	0.49	4.63	19.79	<0.0001
3	$NDVI*PAR_d$	25	0.54	4.40	20.24	<0.0001	26	0.59	4.39	18.76	<0.0001
	$SAVI*PAR_d$	21	0.52	4.29	20.25	<0.0001	24	0.57	4.38	18.73	<0.0001
	$sWDRVI*PAR_d$	25	0.59	4.21	19.40	<0.0001	26	0.58	4.41	18.85	<0.0001
4	*NDVI*LAI*	**25**	**0.70**	**3.56**	**16.38**	**<0.0001**	**26**	**0.79**	**3.14**	**13.42**	**<0.0001**
	*SAVI*LAI*	21	0.63	3.81	17.67	<0.0001	**24**	**0.80**	**3.01**	**12.86**	**<0.0001**
	*sWDRVI*LAI*	25	0.69	3.61	16.61	<0.0001	26	0.73	3.55	15.16	<0.0001
		Spring barley					Potatoes				
1	*LAI*	22	0.65	2.51	17.87	<0.0001	22	0.75	2.18	18.99	<0.0001
2	*NDVI*	25	0.82	1.73	12.33	<0.0001	**22**	**0.91**	**1.26**	**10.94**	**<0.0001**
	SAVI	23	0.81	1.77	12.63	<0.0001	19	0.90	1.40	12.21	<0.0001
	sWDRVI	**25**	**0.86**	**1.55**	**10.99**	**<0.0001**	22	0.85	1.66	14.45	<0.0001
	PRI	21	0.05	3.88	27.24	0.235	21	0.03	4.22	36.75	0.4533
3	$NDVI*PAR_d$	25	0.82	1.70	12.12	<0.0001	22	0.86	1.54	13.43	<0.0001
	$SAVI*PAR_d$	23	0.83	1.66	11.81	<0.0001	19	0.81	1.64	14.26	<0.0001
	$sWDRVI*PAR_d$	25	0.84	1.64	11.69	<0.0001	22	0.79	1.87	16.25	<0.0001
4	*NDVI*LAI*	**22**	**0.83**	**1.79**	**12.70**	<0.0001	22	0.76	2.10	18.30	<0.0001
	*SAVI*LAI*	22	0.78	1.92	13.67	<0.0001	22	0.76	1.99	17.30	<0.0001
	*sWDRVI*LAI*	22	0.81	1.73	12.80	<0.0001	22	0.75	2.12	18.49	<0.0001
		ALL cereals					Cereals + potatoes				
1	*LAI*	74	0.61	4.10	17.09	<0.0001	96	0.65	3.79	15.81	<0.0001
2	*NDVI*	76	0.60	4.09	17.02	<0.0001	98	0.65	3.67	15.29	<0.0001
	SAVI	68	0.54	4.34	18.09	<0.0001	87	0.50	4.38	18.24	<0.0001
	sWDRVI	76	0.62	4.03	16.79	<0.0001	98	0.65	3.74	15.60	<0.0001
	PRI	64	0.37	4.86	20.26	<0.0001	85	0.29	4.98	20.73	<0.0001
3	$NDVI*PAR_d$	76	0.59	4.10	17.10	<0.0001	98	0.61	3.79	15.79	<0.0001
	$SAVI*PAR_d$	68	0.48	4.61	19.19	<0.0001	87	0.39	4.76	19.85	<0.0001
	$sWDRVI*PAR_d$	76	0.58	4.15	17.30	<0.0001	98	0.59	3.88	16.16	<0.0001
4	*NDVI*LAI*	**73**	**0.74**	**3.42**	**14.39**	**<0.0001**	**95**	**0.74**	**3.26**	**13.57**	**<0.0001**
	*SAVI*LAI*	67	0.63	3.87	16.12	<0.0001	89	0.56	4.03	16.79	<0.0001
	*sWDRVI*LAI*	73	0.65	3.88	16.18	<0.0001	99	0.71	3.40	14.16	<0.0001

Notes.

n, number of observations; R^2, coefficient of determination; *RMSE*, root mean square error; *NRMSE*, normalized root mean square error.
The best performing models are in bold print.

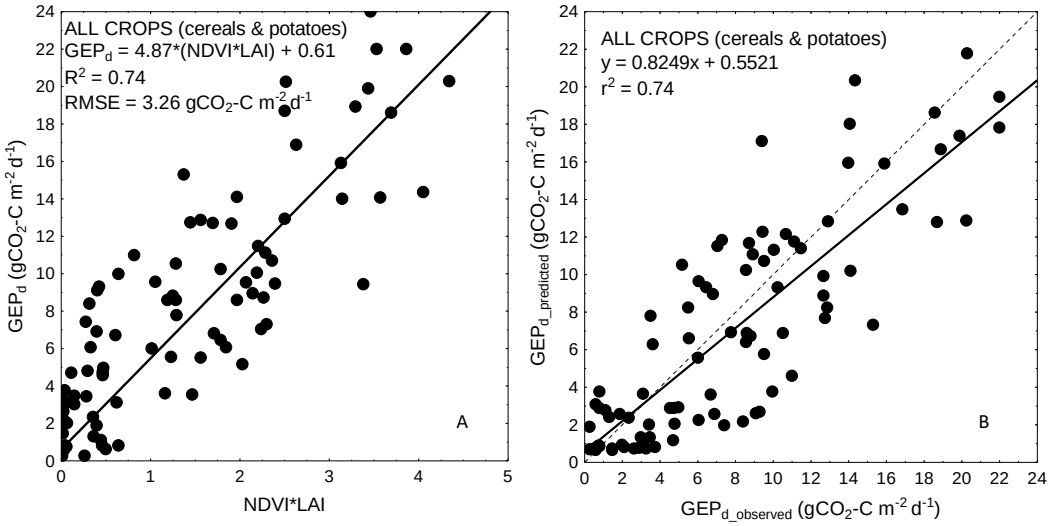

Figure 3 **Scatterplots of relationships between (A) *NDVI*LAI* and GEP_d and (B) observed and predicted GEP_d estimated for all the crops considered together, based on the general crop-combined model.**

Full-size DOI: 10.7717/peerj.5613/fig-3

DISCUSSION

Most of the remote sensing-based models to estimate *GEP* of croplands are rather crop-specific. They were developed for maize, soybean (*Gitelson et al., 2012*), rice (*Inoue et al., 2008*), wheat (*Wu et al., 2009*), rye, barley, potato (*Uździcka et al., 2017*) and in the majority of studies it has not been tested if these models can be directly applied (without reparametrization) for estimation of CO_2 uptake for other crops. Here we presented a more general and robust approach based on combining the datasets for the two winter and two spring crops together and we proved that the accuracy of crop-combined models is not different from those developed for winter crops on a separate basis (NRMSE of the best crop-combined models are in range of 13–16%), but it may be lowered compared to simple *VI*-based models developed for spring barley and potato (NRMSE is in range of about 11% for spring crops, whereas NRMSE of the best crop-combined model is 13.57%, Table 4).

The weakness of our study is related to the applied method for spectral properties measurements. The Spectrosense 2+ measuring system with 4-channel upward- and downward-looking multispectral radiometers allows to measure incident and reflected radiation only in four most commonly used bands (NIR, RED and GREEN wavelengths). Due to missing measurements at red-edge, blue and other specific wavelengths we were not able to calculate many other important indices more sensitive to medium to high biomass (e.g., $NDVI_{\text{red–edge}}$ (*Gitelson & Merzlyak, 1994*), Normalized Difference Structural Index, *NDSI* (*Vescovo et al., 2012*)) or *EVI* (*Huete et al., 2002*), which could help to overcome the saturation effect of classical greenness indices. Besides *NDVI*, which tends to saturate asymptotically under moderate-to-high biomass conditions (*Huete et al., 2002*; *Gitelson et al., 2003*), we analyzed *SAVI*—the index developed to compensate for the reflectance

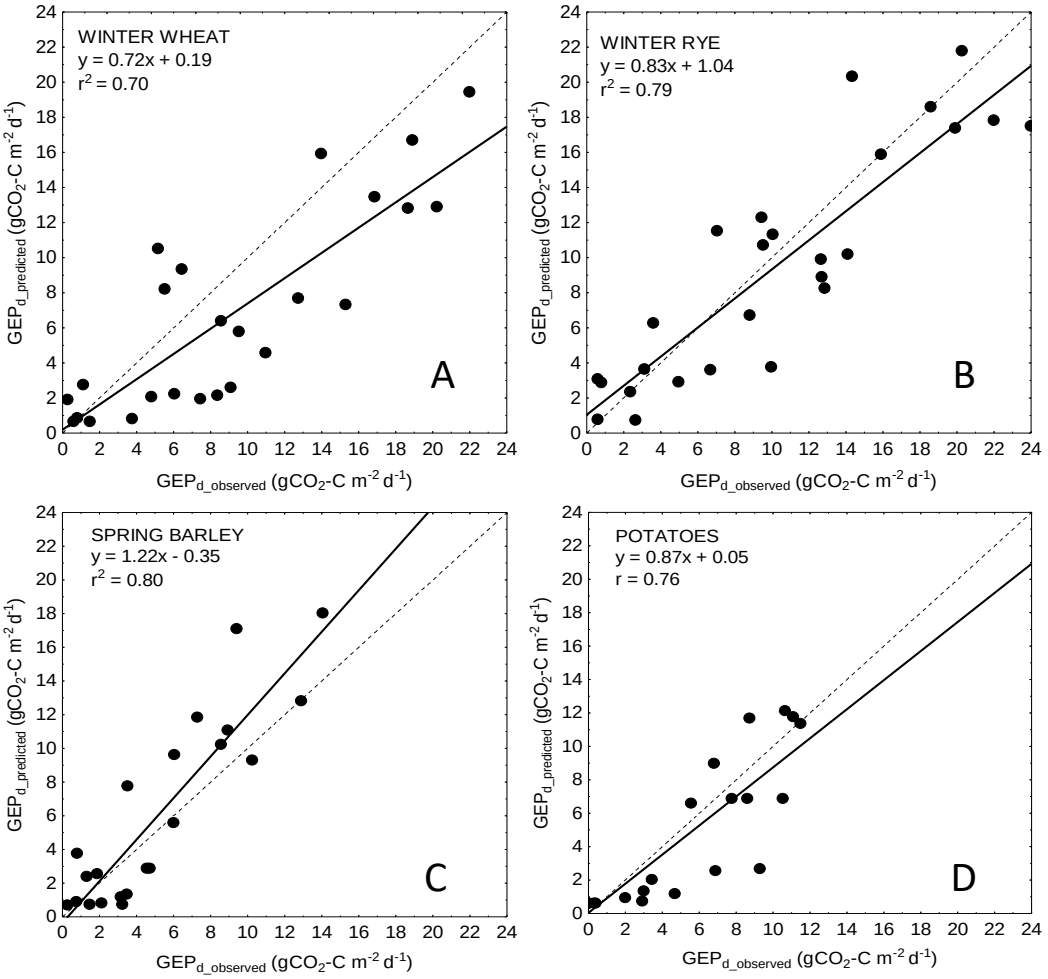

Figure 4 Scatter plots of relationships between observed and predicted GEP_d for the analyzed crops. (A) winter wheat; (B) winter rye; (C) spring barley and (D) potatoes. GEP_d for each crop was estimated based on the general crop-combined model: $GEP_d = 4.87 * (NDVI * LAI) + 0.61$.

Full-size DOI: 10.7717/peerj.5613/fig-4

from soil (*Huete, 1988*), and *WDRVI* which was developed to increase the linearity with biophysical parameters (*Gitelson, 2004*). *SAVI* improved the accuracy of GEP_d estimations only for winter rye (NRMSE of *SAVI* model was smaller by 33% than for *NDVI*-based model), but did not improve the accuracy of GEP_d estimations of neither winter wheat nor spring crops. *WDRVI* improved estimations of GEP_d only for spring barley (NRMSE of *WDRVI* model was smaller by 16% than for *NDVI*-based model), and did not affect the GEP_d model accuracy of other crops (Table 4). *WDRVI* explained maximum 62% of GEP_d variability for winter rye and only 50% for winter wheat and RMSE in both cases was not very much different from *NDVI*- or *SAVI*- based models. In case of spring crops *WDRVI* performed much better and explained around 85–86% of variability in GEP_d for spring barley and potato, respectively, although only for spring barley this index was the

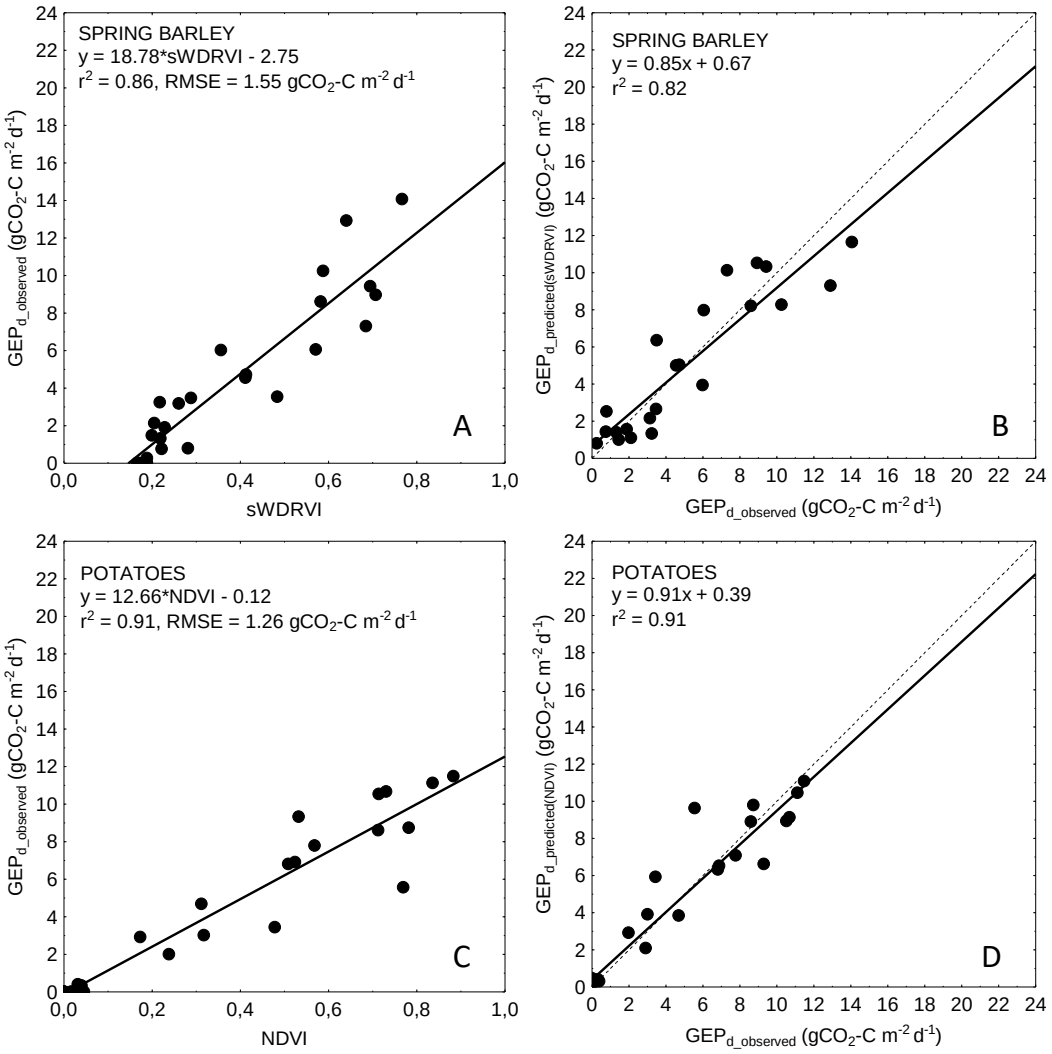

Figure 5 Relationships between the best fitted *VIs* and GEP_d as well as between observed and predicted daily *GEP* for spring barley (A, B) and potatoes (C, D). Predicted GEP_d was calculated based on *VI* model resulting in the best goodness of fit (see Table 4).

Full-size DOI: 10.7717/peerj.5613/fig-5

best proxy of GEP_d (Table 4, Fig. 5). *NDVI* explained even 91% of GEP_d variability of potato being the best predictor of GEP_d.

Inclusion of PAR into *VI*-based models, although successfully implemented in many studies (e.g., *Gitelson et al., 2006*; *Wu et al., 2009*; *Rossini et al., 2010*), did not improve goodness-of-fit of the linear regressions for any of the crops. Similar results have been reported also by *Rossini et al. (2012)* and *Sakowska et al. (2014)* for alpine grassland ecosystems. *Sakowska et al. (2014)* hypothesized that this might be the result of a different response of plant photosynthesis to direct and diffuse radiation, but this cannot support our results, because all measurements were taken under sunny days. As stated by *Rossini et al. (2012)*, although models including PAR and *VI* take into account variations related

to changing incident radiation, they may not improve estimation of *GEP* due to higher light use efficiency (*LUE*) of plants at lower values of incident PAR and lower *LUE* at higher PAR (due to higher photoinhibition). *Rossini et al. (2012)* argued that higher photosynthetic efficiency at low PAR may be the result of two processes: (1) more diffuse light is penetrating more deep into the canopy, and (2) less photoinhibition on the top of the canopy which may reduce tendency towards saturation (*Chen, Shen & Kato, 2009*). It is well known that exposure of photosynthetic machinery of plants to strong light may result in inhibition of the photosystem II (PSII) activity, due to toxic effect of reactive oxygen species (*Murata et al., 2007*). Although this effect may be overcome by rapid and efficient repair of PSII (*Aro, Virgin & Anderson, 1993*), environmental factors, such as e.g., heat stress, which often occur during growing season, may inhibit the reparation of PSII and hence reduce efficiency of CO_2 uptake (*Murata et al., 2007*). This is probably why we observed a very weak correlation between GEP_d and average daily values of incident PAR (Fig. 6). Although GEP_d was increasing with increasing PAR during the vegetative phase of crop development, *LUE* became stable, while *LAI* and biomass of plants have been increasing continuously (Figs. 2 and 6). During the reproductive phase, both GEP_d and *LUE* decreased with decreasing values of PAR_d, but this effect is clearly related to progressive degradation of photosynthetic apparatus towards the senescence. Considering the above, we may hypothesize that the increasing GEP_d observed during the vegetative phase of plant development cycle is mostly related to increasing biomass of plants and amount of photosynthetic apparatus rather than to increasing PAR. Another point is that the chamber measurements of CO_2 fluxes were taken on sunny days, when PAR was not a limiting factor for *GEP*. This is probably why we found a week correlation between GEP_d and average daily PAR, which can indicate that over such a long seasonal time scales PAR is not the most relevant determinant of GEP_d, although in shorter time-scales it may be more important (as indicated also by *Sims et al., 2006*).

One of the possible explanation, why the simple greenness indices considered in this study were moderately correlated with GEP_d of winter crops might be that we considered all the 3-years period dataset together for all the crops, while it is clear that climatological conditions for all these years were extremely different. Especially, 2011- a year with a very dry spring, has disturbed the relationships between GEP_d and *VIs* (mainly for winter crops) and although not shown, the same *VIs*-based models obtained specifically for 2012 and 2013 resulted in a much higher accuracy. However, our intention was to test the multiyear relationships between *VIs* and GEP_d in order to develop more general models which can be applied to years characterized by different climatological conditions, still maintaining a reliable performance.

Another reason for higher uncertainties of GEP_d estimations with *VIs*, observed specifically for winter crops, might be related to seasonal changes in canopy structure and biochemical traits which may modify the spectral response of plants over the growing season at different phenological phases of plant development (*Asrar et al., 1984*; *Asrar, Kanemasu & Yoshida, 1985*; *Peng et al., 2017*). The seasonal courses of GEP_d and *NDVI* are nearly the same and are overlapping for potato (Fig. 7) and that is why the greenness indices (*NDVI, SAVI* and *WDRVI*) are good proxies of GEP_d for this crop (R^2 for GEP_d vs. *VIs*

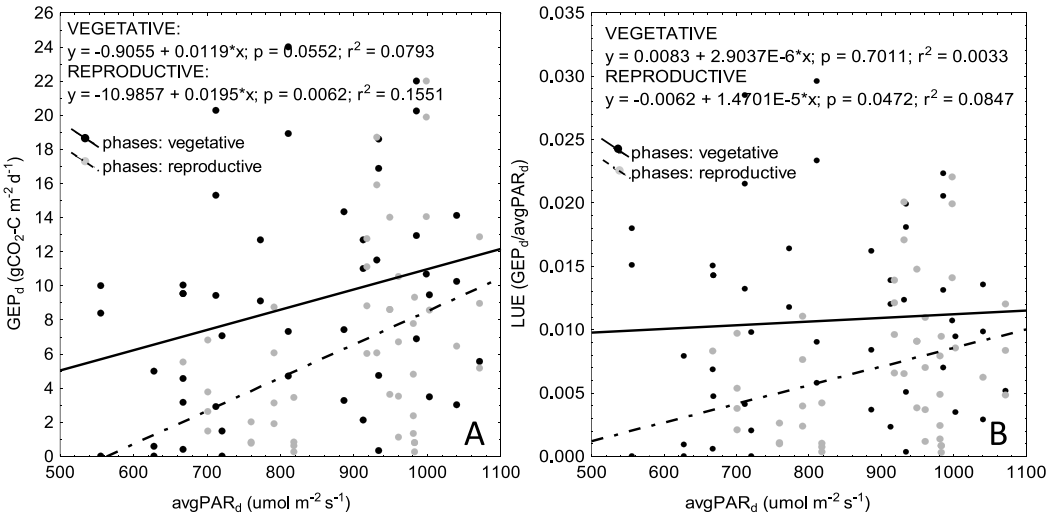

Figure 6 Scatterplots of relationships between average daily PAR (PAR_d) and GEP_d (A) as well as PAR_d and *LUE* (B) for vegetative and reproductive phases of plant development. Data for all the crops are presented on the graphs.

Full-size DOI: 10.7717/peerj.5613/fig-6

relationships of 0.85, 0.90 and 0.91 for *WDRVI, SAVI* and *NDVI* respectively, see Table 4). However, in case of winter crops and spring barley these GEP_d and *NDVI* seasonal courses did not correspond as well as they did for potato. We observed clearly a shift in seasonal courses of *NDVI* and GEP_d for spring barley, winter rye and winter wheat, and peaks of *NDVI* occurred earlier than peaks of GEP_d for all these crops (Fig. 7). It is well known that *NDVI* saturates at moderate-to-high biomass conditions (*Gitelson et al., 2003*), but this effect seems to be crop specific and may depend on the structure of the crop canopy. In spring barley *NDVI* was increasing together with *LAI* and GEP_d until DOY140 (Fig. 7). After this day *NDVI* saturated and stabilized at around 0.8 until DOY165, although GEP_d and *LAI* were already decreasing. For winter wheat, *NDVI* also followed *LAI* development during the vegetative phase (untill DOY140), but until DOY120 the increase rates of *NDVI* were slower and its value did not exceed 0.4 since the beginning of the growing season, while GEP_d increased much faster during this period. Hence, we can hypothesize that GEP_d *vs. NDVI* relationships might be different in the period between DOY80 to DOY120 and between DOY120 to DOY140, although we cannot confirm this due to not sufficient amount of data. After DOY140, *NDVI* saturated and stabilized again at around 0.8 until DOY165 and just after it begun to decrease slowly and the rate of decreasing was the same as the rate of GEP_d decrease. Hence, in the reproductive/senescence phase of wheat development from DOY165 till the harvest, again GEP_d *vs. NDVI* relationships were significantly ($p < 0.05$) different (Fig. 8). Much more complex analysis are related to winter rye, where *NDVI* reached maximum values of around 0.9 very soon after the beginning of the analyzed period and was quite stable until DOY140, although *LAI* and GEP_d were continuously increasing until DOY145. When analyzing the winter crop data, specifically winter rye, one should take into account that this crop is sawn in the late September under

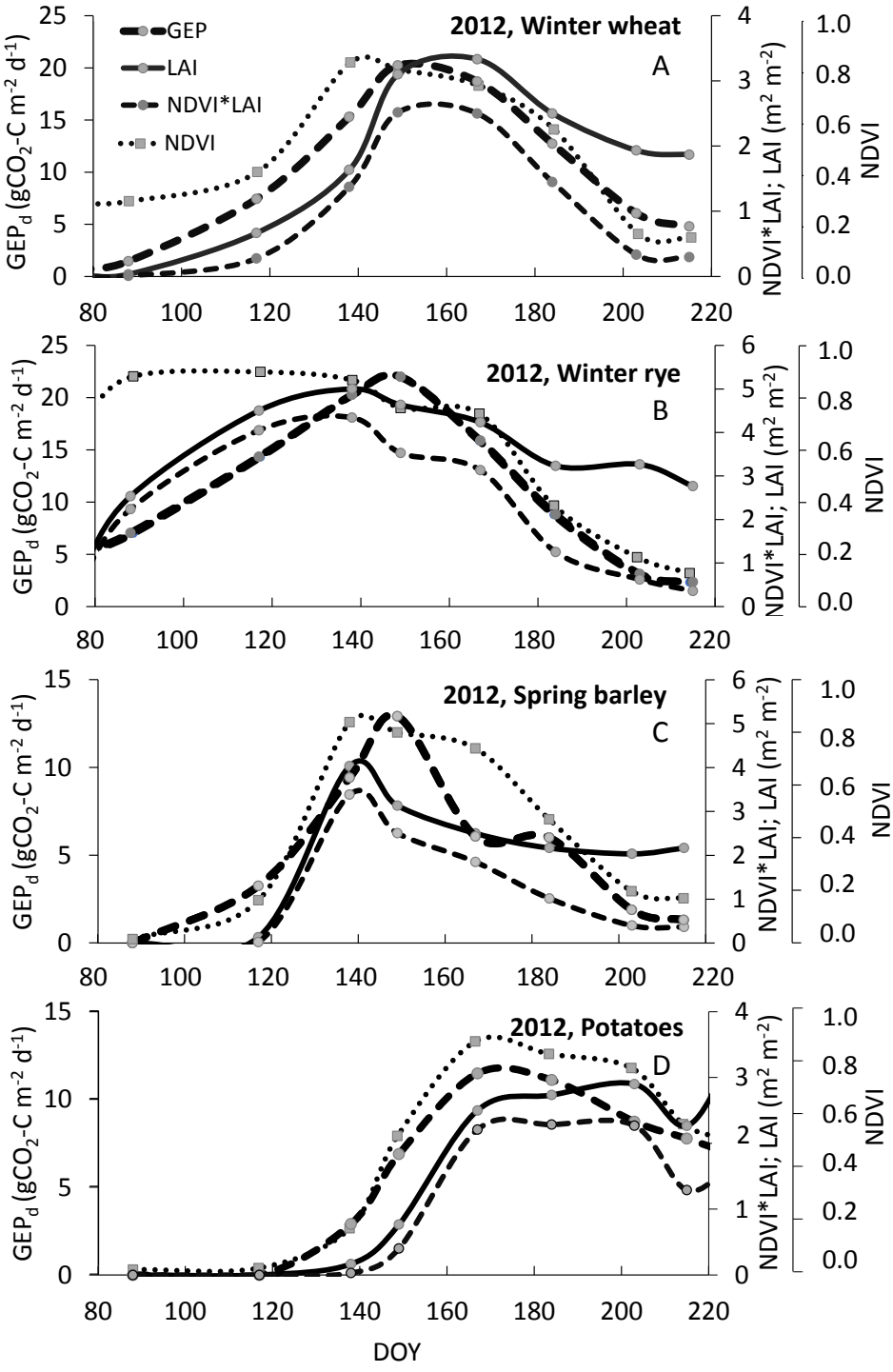

Figure 7 **Example of seasonal courses of *GEP$_d$*, *NDVI*, *LAI* and *NDVI*LAI* for winter wheat (A), winter rye (B), spring barley (C) and potato (D) in 2012.** Note: scales are different.

Full-size DOI: 10.7717/peerj.5613/fig-7

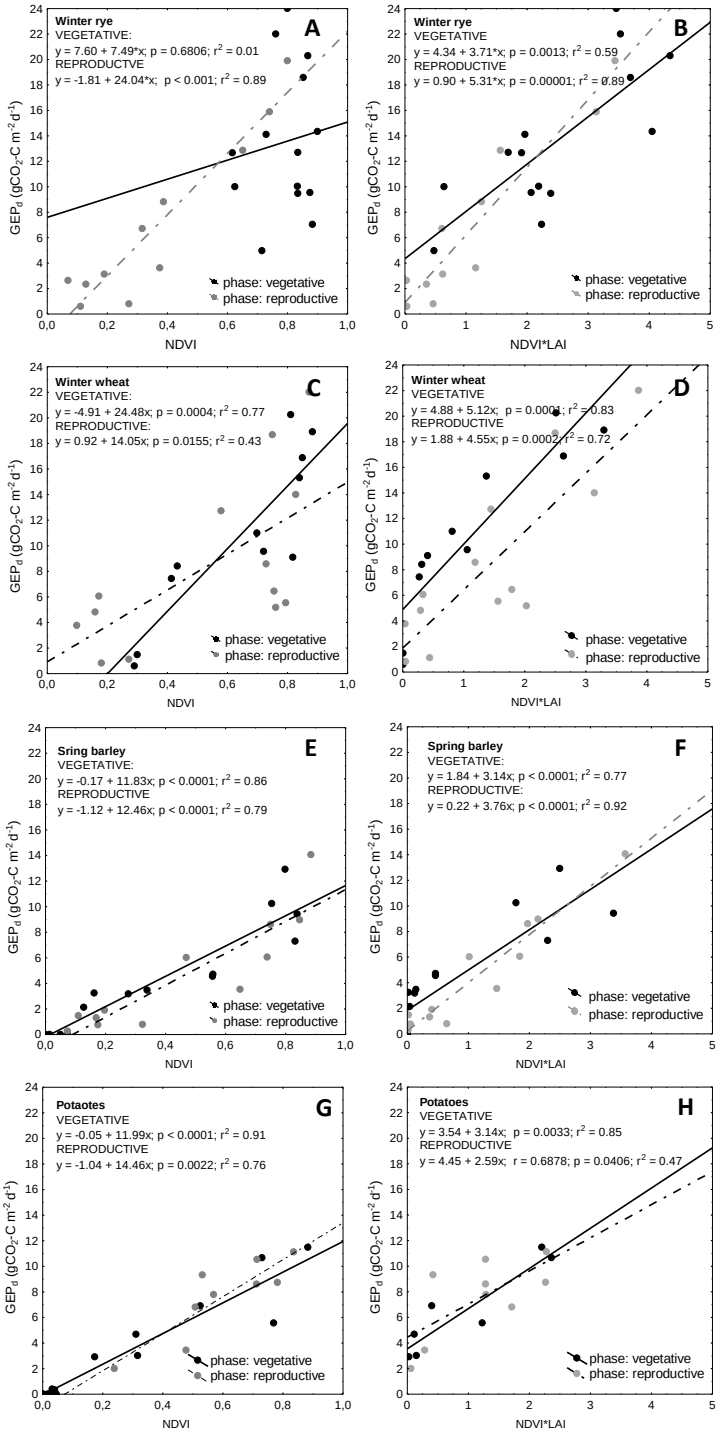

Figure 8 Scatterplots of relationships between *NDVI* and GEP_d as well as between *NDVI*LAI* and GEP_d for the analyzed crops. (A and B) winter rye; (C and D) winter wheat; (E and F) spring barley; and (G and H) potato. Relationships are determined for vegetative and reproductive phases of plant development cycle.

Full-size DOI: 10.7717/peerj.5613/fig-8

the climatic conditions of the Central Europe and during warm winters it can continue to grow. In early spring, after the beginning of the growing period, the canopy of the crop may get very dense and green if it is growing under non N-limited conditions. In our case, the winter of 2012 was warmer than in 2011 and 2013, with a very warm December and January 2012 (Fig. 1), hence crops continued to grow during this time. Considering above, this may explain why *NDVI* saturated already in the late March/beginning of April 2012 at winter rye fields (Fig. 7). In 2011 and 2013 this effect was also observed, but beginning of the period when *NDVI* started to saturate occurred one month later (in April), due to longer and colder winters. For the first part of the growing season of 2012 for the winter rye, *NDVI* was not sensitive to changes neither in biomass, nor in GEP_d (the same was observed in all the three analyzed years, data shown in (File S7). Between DOY160 and the harvest, changes of *NDVI* followed changes of GEP_d, but again the GEP_d *vs. NDVI* relationships were significantly ($p < 0.05$) different than those found for vegetative phase (Fig. 8).

Similar kind of hysteresis were found in relationships between GEP_d and *LAI* and GEP_d vs. chlorophyll content in maize by *Gitelson et al. (2014)*, as well as between reflectance in red and blue bands and greenness indices (e.g., *NDVI*) vs. chlorophyll content in maize and soybean by *Peng et al. (2017)*. The relationships between these variables were significantly different for vegetative and reproductive phases of maize and soybean development. In our study we found similar kind of differences between GEP_d and *NDVI* in both analyzed winter crops, but not in spring barley and potato. Each of the crops has different height, *LAI,* canopy architecture, and different contribution of soil to canopy reflectance. As already indicated e.g., by *Gausman et al. (1971)* and *Gausman, Rodriguez & Richardson (1976)*, and discussed by *Peng et al. (2017)*, optical properties of leaf and canopies are greatly impacted by leaf structure and canopy architecture and that is why relationships between biophysical properties of crops and *VIs* are often different at different phenological phases of plant development (*Asrar et al., 1984*; *Asrar, Kanemasu & Yoshida, 1985*; *Gitelson et al., 2014*). In winter crops the canopy is very green, dense and more "closed" at the beginning of the growing season and hence reflectance from soil is minimized, while absorption in the red part of the spectrum is high. That is why *NDVI* saturates early in the season and it does not change much over the vegetative phase of crop development. Whereas in the reproductive/senescence phases, when the leaf structure and canopy architecture change and chlorophyll content is reduced, more light can penetrate deeper into the canopy and that is why the soil reflectance contribution is also higher. Due to differences in canopy architecture and leaf structure and different patterns of light absorption and reflectance by crops as well as different contribution of soil into overall reflectance of vegetation canopies at different phases of phenological development of plants, the relationships between GEP_d and *VIs* of winter crops are different for vegetative and reproductive phases, as indicated also by (*Peng et al., 2017*; *Gitelson et al., 2014*). In potato, canopy is more open since the beginning of the growing season, and soil reflectance contributes significantly to the overall canopy reflectance. With the development of the green biomass, absorption of the red part of the spectrum is increasing, while soil contribution is decreasing. After the peak of biomass, during the reproductive and senescence phases, when chlorophyll pigments are

degrading while leaves are folding, more light penetrates deeper to the canopy and again contribution of the soil reflectance to the overall canopy reflectance increases, whereas absorption in the red part of the spectrum decreases. Probably this effect can cause lack of hysteresis in GEP_d *vs. NDVI* relationships for this crop, as the slopes of curves for this relationships in both phases of potato development are the same (Fig. 8).

In winter crops, *LAI* started to increase since the beginning of the growing season throughout the vegetative phase and GEP_d followed changes in the crop biomass, although *NDVI* was already not sensitive enough to track changes in photosynthesis. The same *LAI* development was found in spring barley and potato, however *NDVI* followed changes in *LAI* and as discussed above, it was sensitive enough to track changes in GEP_d of spring crops. After the peak of biomass, *LAI* of all the crops decreased slightly and stabilized at around 2–3 m^2 m^{-2} until the harvest (note, we are not investigating *greenLAI*, but total *LAI*). This led to the conclusion, that *LAI* can be successfully used to overcome problems with greenness indices, which seem to saturate very early in the growing season in winter crops. By multiplication of *NDVI*-based *VIs* by *LAI* this specific issue of seasonal GEP_d *vs. VIs* relationships can be overcome and model uncertainties can be reduced (see Table 4). The curves presenting the seasonal variations of the *NDVI*LAI* product are more closely related to seasonal changes in GEP_d (Fig. 7) and this effect is not only restricted to winter crops, but can also be observed in case of spring crops. For both winter crops the slopes of the GEP_d vs. *NDVI* relationships are significantly different ($p < 0.05$) between vegetative and reproductive phases and between the species, which can limit their application for accurate estimation of GEP_d of these canopies over the entire season (Fig. 8). However, after multiplying *NDVI* by *LAI* slopes for the same relationships are much closer to each other (Fig. 8), and uncertainties of GEP_d estimations are lower, as indicated in Table 4. Moreover, this approach does not change significantly slopes of the GEP_d vs. *NDVI* relationships for spring crops (Fig. 8), although uncertainties of GEP_d estimations for potato can be higher (Table 4).

However, in the more general, crop-combined dataset representing both winter and spring crops, the multiplication of *NDVI* and *LAI* led to an improvement of GEP_d estimations (Table 4). NRMSE for the model fed with *NDVI*LAI* was about 14%, and it explained around 74% of GEP_d variability independently from the crop species. The obtained accuracy is in the range which can promote this approach in remote sensing studies in order to overcome the hysteresis of GEP_d *vs. VIs* relationship between vegetative and reproductive phases, which indeed may limit their applicability to predict photosynthesis of different crops over the entire growing season.

The limitation of this approach is that *VIs* are the remote sensing source of information which can be obtained from space, while space born products of *LAI* are result of (1) statistical models which quantify the relationships between *LAI* and canopy reflectance or *VIs* (*Baret & Guyot, 1991*; *Verrelst et al., 2015*; *Linker & Gitelson, 2017*), or (2) different radiative transfer models (*Baret et al., 2007*; *Richter et al., 2012*). These relationships between *LAI* and *VIs* are often canopy structure- and land-cover depended and are highly impacted by leaf angle distribution, vegetation clumping, optical properties of leaf and canopies (*Goward & Huemmrich, 1992*). What is more, different canopies may exhibit large

variations in reflectance properties which can result in different values of *VIs* for similar values of *LAI* and other biophysical parameters (*Pinty, Leprieur & Verstraete, 1993*). There are few satellite based products of *LAI* (*Zheng & Moskal, 2009*) which are based not only on single vegetation indices such as *EVI* (*Huete et al., 2002*) or Reduced Simple Ratio (*RSR*, *Brown et al., 2000*), but also on linear or non-liner models including many vegetation indices which are used to estimate and map *LAI* at the landscape and global levels with Landsat satellites (*Cohen, Maierspergerr & Tumer, 2003*). Hence, we believe that this kind of data (*LAI* retrieved from space borne data) can also be used to mitigate the hysteresis effect described above and increase the accuracy of GEP_d estimations for croplands. We can even speculate, considering that *greenLAI* and total *LAI* analyzed in this study are the same in the vegetative phase of plant development, while *greenLAI* is decreasing till "zero" in the senescence phase, although the total *LAI* remains relatively constant during this phase, that the product of *NDVI* and *greenLAI* retrieved from satellite data will improve estimations of GEP_d of winter crops even better than total *LAI* used in this study. *GreenLAI* multiplied by greenness related *VIs* shall improve model accuracy both in the vegetative and reproductive phases of plant development cycle, due to reasons described above. Hence, we hypothesize that the overall hysteresis effect observed in relationships between greenness related *VIs* and *GEP* will be reduced. However, this effect will need to be studied in the future in more detail with the application of both *greenLAI* estimated at the ground and based on satellites data.

The proposed approach and empirical models developed in this study can be tested in other regions and for other C3 crops in order to verify the validity of our assumptions. Considering that our models were developed based on four different crops and three years characterized by different climatic conditions we believe that application of the proposed approaches and formulas can result in reliable estimation of daily *GEP* values of crops also for other regions with similar climate and crop management systems.

CONCLUSIONS

The analyzed multiyear relationships between GEP_d and *VIs* showed that only in the case of spring crops GEP_d can be estimated with a high accuracy and with an error smaller than 12% based on simple greenness indices (*NDVI, SAVI, WDRVI*). The same kind of analyzes conducted for winter crops are much less accurate, and the error of GEP_d estimation is higher than 18%.

The reason for the weaker correlation between daily *GEP* and *VIs* of winter crops may be related to hysteresis effect of this relationship found between the vegetative and reproductive phases of plant development cycle. We found that multiplication of greenness indices by *LAI* (which is much more sensitive to changes in biomass and GEP_d of winter crops, specifically during the vegetative phase of their development) can mitigate such effect. The product of multiplication of *LAI* and *VI* has in most cases the same seasonality as GEP_d and that is why it represents well the seasonal changes of gross CO_2 fluxes of croplands.

In order to propose as universal model as possible, we investigated the relationships between *VIs* and GEP_d for the cereals- and crop-combined datasets, where both winter

and spring crops, as well as cereals and potato were included. We found that there is no difference in GEP_d estimations between these two kind of approaches and this general model based on approach where *NDVI* is multiplied by *LAI*, can be successfully applied for both winter and spring crops as well as for cereals and potato, while the error of this estimation is not higher than 14%. However, this approach underestimated GEP_d of winter crops and potatoes, and overestimated GEP_d of spring barley, but the rate of over-or under-estimations was not higher than 25%.

ACKNOWLEDGEMENTS

The authors sincerely thank Prof. Andrzej Blecharczyk and Dr. Wojciech Waniorek from Agronomy Department (AD) of Poznan University of Life Sciences for their support in implementing our study on fields of the long-term experimental farm of AD in Brody. We would like to thank Jędrzej Nyćkowiak, Klaudia Ziemblińska, Krzysztof Ławiński and Daria Polmańska for their help in CO_2 chamber measurements and Anna Binczewska for the help in reflectance and LAI measurements. We would like to thank Dr. Anshu Rastogi for his comments to the manuscript and anonymous reviewers for all valuable suggestions which helped to improve the quality of the revised manuscript.

ADDITIONAL INFORMATION AND DECLARATIONS

Funding

The measurements were funded by the Polish Ministry of Science under project No. 752/1/N-COST-2 010-0 "Assessment of the temporal and spatial variation of the biophysical and spectral indices (NDVI, PRI, WBI) in reference to net exchange of CO_2, CH_4, H_2O between different ecosystems (peatland, forest and arable) and the atmosphere". During data processing and manuscript writing, Radosław Juszczak was supported by project No. 2016/21/B/ST10/02271 funded by the National Science Centre of Poland. This project has received funding also from the European Union's Horizon 2020 research and innovation programme under the Marie Skłodowska-Curie Grant Agreement No. 749323. There was no additional external funding received for this study. The funders had no role in study design, data collection and analysis, decision to publish, or preparation of the manuscript.

Grant Disclosures

The following grant information was disclosed by the authors:
Polish Ministry of Science: 752/1/N-COST-2 010-0.
National Science Centre of Poland: 2016/21/B/ST10/02271.
European Union's Horizon 2020 research and innovation programme under the Marie Skłodowska-Curie Grant Agreement: 749323.

Competing Interests

The authors declare there are no competing interests.

Author Contributions

- Radosław Juszczak conceived and designed the experiments, performed the experiments, analyzed the data, contributed reagents/materials/analysis tools, prepared figures and/or tables, authored or reviewed drafts of the paper, approved the final draft.
- Bogna Uździcka performed the experiments, analyzed the data, contributed reagents/materials/analysis tools, prepared figures and/or tables, authored or reviewed drafts of the paper.
- Marcin Stróżecki performed the experiments, approved the final draft.
- Karolina Sakowska performed the experiments, authored or reviewed drafts of the paper, approved the final draft.

Data Availability

The following information was supplied regarding data availability:

The raw data are provided in the Supplemental Files.

Supplemental Information

Supplemental information for this article can be found online at http://dx.doi.org/10.7717/peerj.5613#supplemental-information.

REFERENCES

Acosta M, Juszczak R, Chojnicki B, Pavelka M, Havránková K, Lesny J, Krupková L, Urbaniak M, Machačová K, Olejnik J. 2017. CO_2 fluxes from different vegetation communities on a peatland ecosystem. *Wetlands* **37(3)**:423–435 DOI 10.1007/s13157-017-0878-4.

Aro EM, Virgin I, Anderson B. 1993. Photoinhibition of photosystem II. Inactivation, protein damage and turnover. *Biochimica et Biophysica Acta* **1143**:113–134 DOI 10.1016/0005-2728(93)90134-2.

Asrar G, Fuchs M, Kanemasu ET, Hatfield JL. 1984. Estimation absorbed photosynthetic radiation and leaf area index from spectral reflectance in wheat. *Agronomy Journal* **76**:300–306 DOI 10.2134/agronj1984.00021962007600020029x.

Asrar G, Kanemasu ET, Yoshida M. 1985. Estimates of leaf area index from spectral reflectance of wheat under different cultural practices and solar angle. *Remote Sensing of Environment* **17**:1–11 DOI 10.1016/0034-4257(85)90108-7.

Baldocchi DD, Falge E, Gu L, Olson R, Hollinger D, Running S, Anthoni P, Bernhofer CH, Davis K, Evans R, Fuentes J, Goldstein A, Katul G, Law B, Lee X, Malhi Y, Meyers T, Munger W, Oechel W, Paw UKT, Pilegaard K, Schmid HP, Valentini R, Verma S, Vesela T, Wilson K, Wofsy S. 2001. FLUXNET: a new tool to study the temporal and spatial variability of ecosystem-scale carbon dioxide, water vapor, and energy flux densities. *Bulletin of the American Meteorology Society* **82(11)**:2415–2434 DOI 10.1175/1520-0477(2001)082<2415:FANTTS>2.3.CO;2.

Baret F, Guyot G. 1991. Potentials and limits of vegetation indices for LAI and APAR assessment. *Remote Sensing of Environment* **35**:161–173 DOI 10.1016/0034-4257(91)90009-U.

Baret F, Hagolle O, Geiger B, Bicheron P, Miras B, Huc M, Berthelot B, Niño F, Weiss M, Samain O, Roujean JL, Leroy M. 2007. LAI, fAPAR, and fCover CYCLOPES global products derived from VEGETATION Part 1: principles of the algorithm. *Remote Sensing of Environment* **110**:275–286 DOI 10.1016/j.rse.2007.02.018.

Blecharczyk A, Sawińska Z, Małecka I, Sparks TH, Tryjanowski. 2016. The phenology of winter rye in Poland: an analysis of long-term experiment data. *International Journal of Biometeorology* **60**:1341–1346 DOI 10.1007/s00484-015-1127-2.

Borge NH, Leblanc E. 2001. Comparing prediction power and stability of broad-band and hyperspectral vegetation indices for estimation of green leaf area index and canopy chlorophyll density. *Remote Sensing of Environment* **76**:156–172 DOI 10.1016/S0034-4257(00)00197-8.

Breda NJJ. 2003. Ground-based measurements of leaf area index: a review of methods, instruments and current controversies. *Journal of Experimental Botany* **54(392)**:2403–2417 DOI 10.1093/jxb/erg263.

Brown L, Chen JM, Leblanc SG, Cihlar JA. 2000. A shortwave infrared modification to the simple ratio for LAI retrieval in boreal forests: an image and model analysis. *Remote Sensing of Environment* **71**:16–25 DOI 10.1016/S0034-4257(99)00035-8.

Chen JM, Cihlar J. 1996. Retrieving leaf area index of boreal conifer forests using Landsat TM images. *Remote Sensing Environment* **55**:153–162 DOI 10.1016/0034-4257(95)00195-6.

Chen J, Shen M, Kato T. 2009. Diurnal and seasonal variations in light-use efficiency in an alpine meadow ecosystem: causes and implications for remote sensing. *Journal of Plant Ecology* **2**:173–185 DOI 10.1093/jpe/rtp020.

Cheng Y-B, Zhang Q, Lyapustin AI, Wang Y, Middleton EM. 2014. Impacts of light use efficiency and fPAR parameterization on gross primary production modeling. *Agricultural and Forest Meteorology* **189–190**:187–197 DOI 10.1016/j.agrformet.2014.01.006.

Chojnicki BH. 2013. Spectral estimation of wetland carbon dioxide exchange. *International Agrophysics* **27**:1–5 DOI 10.2478/v10247-012-0061-3.

Chojnicki B, Michalak M, Acosta M, Juszczak R, Augustin J, Droesler M, Olejnik J. 2010. Measurements of carbon dioxide fluxes by chamber method at the Rzecin wetland ecosystem, Poland. *Polish Journal of Environmental Studies* **19**:283–291.

Cohen WB, Maierspergerr TK, Tumer DP. 2003. An improved strategy for regression of biophysical variables and Landsat ETM+ data. *Remote Sensing of Environment* **84**:561–571 DOI 10.1016/S0034-4257(02)00173-6.

Drösler M. 2005. Trace gas exchange and climatic relevance of bog ecosystem, Southern Germany. PhD Dissertation, Lehrstuhl für Vegetationsokologie, Department für Ökologie, Technischen Universität München.

Gamon JA, Penuelas J, Field CB. 1992. A narrow-waveband spectral index that tracks diurnal changes in photosynthetic efficiency. *Remote Sensing of Environment* **41**:35–44 DOI 10.1016/0034-4257(92)90059-S.

Gao F, Anderson MC, Zhang X, Yang X, Alfieri J, Kustas WP, Mueller R, Johnson DM, Prueger JH. 2017. Toward mapping crop progress at field scales trough

fusion of Landsat and MODIS imagery. *Remote Sensing of Environment* **188**:9–25 DOI 10.1016/j.rse.2016.11.004.

Gausman HW, Allen WA, Cardenas R, Richardson AJ. 1971. Effects of leaf nodal position on absorption and scattering coefficients and infinite reflectance of cotton leaves *Gossypium hirsutum L. Agronomy Journal* **63**:87–91 DOI 10.2134/agronj1971.00021962006300010027x.

Gausman HW, Rodriguez RR, Richardson AJ. 1976. Infinite reflectance of dead compared with live vegetation. *Agronomy Journal* **68**:295–296 DOI 10.2134/agronj1976.00021962006800020023x.

Gitelson AA. 2004. Wide dynamic range vegetation index for remote quantification of crop biophysical 643 characteristics. *Journal of Plant Physiology* **161**:165–173 DOI 10.1078/0176-1617-01176.

Gitelson AA, Gamon J, Solovchenko A. 2017. Multiply drivers of seasonal change in PRI: implications for photosynthesis 2.Stand level. *Remote Sensing of Environment* **190**:198–206 DOI 10.1016/j.rse.2016.12.015.

Gitelson A, Merzlyak MN. 1994. Quantitative experiments estimation of chlorophyll-a using reflectance spectra: experiments with autumn chestnut and maple leaves. *Journal of Photochemistry and Photobiology B Biology* **22**:247–252 DOI 10.1016/1011-1344(93)06963-4.

Gitelson AA, Peng Y, Arkebauer TJ, Schepers J. 2014. Relationships between gross primary production, green LAI, and canopy chlorophyll content in maize: implications for remote sensing of primary production. *Remote Sensing of Environment* **144**:65–72 DOI 10.1016/j.rse.2014.01.004.

Gitelson AA, Peng Y, Masek JG, Rundquist D, Verma S, Suyker A, Baker JM, Hatfield JL, Meyers T. 2012. Remote estimation of crop gross primary production with Landsat data. *Remote Sensing of Environment* **121**:404–414 DOI 10.1016/j.rse.2012.02.017.

Gitelson AA, Viña A, Arkebauer TJ, Rundquist DC, Keydan G, Leavitt B. 2003. Remote estimation of leaf area index and green leaf biomass in maize canopies. *Geophysical Research Letters* **30(5)**:1248 DOI 10.1029/2002GL016450.

Gitelson AA, Viña A, Rundquist DC, Ciganda V, Arkebauer TJ. 2005. Remote estimation of canopy chlorophyll content in crops. *Geophysical Research Letters* **32**:L08403 DOI 10.1029/2005GL022688.

Gitelson AA, Viña A, Verma SB, Rundquist DC, Arkebauer TJ, Keydan G, Leavitt B, Ciganda V, Burba GG, Suyker AE. 2006. Relationship between gross primary production and chlorophyll content in crops: implications for the synoptic monitoring of vegetation productivity. *Journal of Geophysical Research* **111**:D08S11 DOI 10.1029/2005JD006017.

Glenn EP, Huete AR, Nagler PL, Nelson SG. 2008. Relationship between Remotely-sensed Vegetation Indices, canopy attributes and plant physiological processes: what vegetation indices can and cannot tell us about the landscape. *Sensors* **8**:2136–2160 DOI 10.3390/s8042136.

Goerner A, Reichstein M, Tomelleri E, Hanan N, Rambal S, Papale D, Dragoni D, Schmullius C. 2011. Remote sensing of ecosystem light use efficiency with MODIS-based PRI. *Biogeosciences* **8**:189–202 DOI 10.5194/bg-8-189-2011.

Goward SN, Huemmrich KF. 1992. Vegetation canopy PAR absorbance and the normalized difference vegetation index: an assessment using the SAIL model. *Remote Sensing of Environment* **39**:119–140 DOI 10.1016/0034-4257(92)90131-3.

Gower ST, Kucharik CJ, Norman JM. 1999. Direct and indirect estimation of leaf area index, fAPAR and net primary production of terrestrial ecosystems. *Remote Sensing of Environment* **70**:29–51 DOI 10.1016/S0034-4257(99)00056-5.

Hassan QK, Bourque CPA, Meng FR. 2006. Estimation of daytime net ecosystem CO_2 exchange over balsam fir forests in eastern Canada: combining averaged tower-based flux measurements with remotely sensed MODIS data. *Canadian Journal of Remote Sensing* **32**:405–416 DOI 10.5589/m07-009.

Hoffman M, Jurisch N, Borraz EA, Hagemann U, Droesler M, Sommer M, Augustin J. 2015. Automated modeling of CO_2 fluxes based on periodic closed chamber measurements. A standardized conceptual and practical approach. *Agricultural and Forest Meteorology* **200**:30–45 DOI 10.1016/j.agrformet.2014.09.005.

Huete AR. 1988. A Soil-Adjusted Vegetation Index (SAVI). *Remote Sensing of Environment* **25**:295–309 DOI 10.1016/0034-4257(88)90106-X.

Huete AR, Didan K, Miura T, Rodriguez E, Gao X, Ferreira L. 2002. Overview of the radiometric and biophysical performance of the MODIS vegetation indices. *Remote Sensing of Environment* **83**:195–213 DOI 10.1016/S0034-4257(02)00096-2.

Hunt ER. 1994. Relationship between woody biomass and PAR conversion efficiency for estimating net primary production from NDVI. *International Journal of Remote Sensing* **15**:1725–1730 DOI 10.1080/01431169408954203.

Inoue Y, Peñuelas J, Miyata A, Mano M. 2008. Normalized difference spectral indices for estimating photosynthetic efficiency and capacity at a canopy scale derived from hyperspectral and CO_2 flux measurements in rice. *Remote Sensing of Environment* **112**:156–172 DOI 10.1016/j.rse.2007.04.011.

Juszczak R, Acosta M, Olejnik J. 2012. Comparison of daytime and nighttime Ecosystem Respiration measured by the closed chamber technique on a temperate mire in Poland. *Polish Journal of Environmental Studies* **21**:643–658.

Juszczak R, Humphreys E, Acosta M, Michalak-Galczewska M, Kayzer D, Olejnik J. 2013. Ecosystem respiration in a heterogeneous temperate peatland and its sensitivity to peat temperature and water table depth. *Plant and Soil* **366**:505–520 DOI 10.1007/s11104-012-1441-y.

Keyser AR, Kimball JS, Nemani RR, Running SW. 2000. Simulating the effect of climate change in the carbon balance of North American high-latitude forests. *Global Change Biology* **6**:185–195 DOI 10.1046/j.1365-2486.2000.06020.x.

Kira O, Nguy-Robertson AL, Arkebauer TJ, Linker R, Gitelson A. 2017. Towards generic models for green LAI estimation in Maize and Soybean: satellite observations. *Remote Sensing 9* **318**:2–16 DOI 10.3390/rs9040318.

Law BE, Falge E, Gu L, Baldocchi DD, Bakwin P, Berbigier P, Davis K, Dolman AJ, Falk M, Fuentes JD, Goldstein A, Granier A, Grelle A, Hollinger D, Janssens IA, Jarvis P, Jensen NO, Katul G, Mahli Y, Matteucci G, Meyers T, Monson R, Munger W, Oechel W, Olson R, Pilegaard K, Paw UKT, Thorgeirsson H, Valentini R, Verma S, Vesala T, Wilson K, Wofsy S. 2002. Environmental controls over carbon dioxide and water vapor exchange of terrestrial vegetation. *Agricultural and Forest Meteorology* **113**:97–120 DOI 10.1016/S0168-1923(02)00104-1.

Law BE, Waring RH. 1994. Remote sensing of leaf area index and radiation intercepted by understory vegetation. *Ecological Applications* **4**:272–279 DOI 10.2307/1941933.

Lloyd J, Taylor JA. 1994. On the temperature dependence of soil respiration. *Functional Ecology* **8**:315–323 DOI 10.2307/2389824.

Majchrzak L, Sawinska Z, Natywa M, Sprzypczak G, Głowicka-Wołoszyn R. 2016. Impact of different tillage systems on soil dehydrogenase activity and spring wheat infection. *Journal of Agricultural Science and Technology* **18**:1871–1881.

Michaelis L, Menten ML. 1913. Die Kinetik der Invertinwirkung. *Biochemistry* **49**:333–369.

Murata N, Takahashi S, Nishiyama Y, Allakhverdiev SI. 2007. Photoinhibition of photosystem II under environmental stress review. *Biochimica et Biophysica Acta* **1767**:414–421 DOI 10.1016/j.bbabio.2006.11.019.

Paruelo JM, Epstein HE, Lauenroth WK, Burke IC. 1997. A NPP Estimates from NDVI for the Central Grassland Region of the United States. *Ecology* **78**:953–958 DOI 10.1890/0012-9658(1997)078[0953:AEFNFT]2.0.CO;2.

Peng Y, Gitelson AA, Keydan G, Rundquist DC, Moses W. 2011. Remote estimation of gross primary production in maize and support for a new paradigm based on total crop chlorophyll content. *Remote Sensing of Environment* **115**:978–989 DOI 10.1016/j.rse.2010.12.001.

Peng Y, Nguy-Robertson A, Arkebauer T, Gitelson AA. 2017. Assessment of canopy chlorophyll content retrieval in maize and soybean: implications of hysteresis on the development of generic algorithms. *Remote Sensing* **9**:226 DOI 10.3390/rs9030226.

Penuelas J, Filella I, Gamon JA. 1995. Assessment of photosynthetic radiation-use efficiency with spectral reflectance. *New Phytology* **131**:291–296 DOI 10.1111/j.1469-8137.1995.tb03064.x.

Pinty B, Leprieur C, Verstraete MM. 1993. Towards a quantitative interpretation of vegetation indices, part1: biophysical canopy properties and classical indices. *Remote Sensing of Environment* **7**:127–150 DOI 10.1080/02757259309532171.

Prince SD, Goward SN. 1995. Global primary production: a remote sensing approach. *Journal of Biogeography* **22**:815–835 DOI 10.2307/2845983.

Propastin P, Kappas M. 2009. Modeling net ecosystem exchange for grassland in central kazakhstan by combining remote sensing and field data. *Remote Sensing* **1**:159–183 DOI 10.3390/rs1030159.

Rahman AF, Sims DA, Cordova VD, El-Masri BZ. 2005. Potential of MODIS EVI and surface temperature for directly estimating per-pixel ecosystem C fluxes. *Geophysical Research Letters* **32**:L19404 DOI 10.1029/2005GL024127.

Richter K, Hank TB, Vuolo F, Mauser W, D'Urso G. 2012. Optimal exploitation of the sentinel-2 spectral capabilities for crop leaf area index mapping. *Remote Sensing* **4**:561–582 DOI 10.3390/rs4030561.

Rossini M, Cogliati S, Meroni M, Migliavacca M, Galvagno M, Busetto L, Cremonese E, Julitta T, Siniscalco C, Morra di Cella U, Colombo R. 2012. Remote sensing-based estimation of gross primary production in a subalpine grassland. *Biogeosciences* **9**:2565–2584 DOI 10.5194/bg-9-2565-2012.

Rossini M, Meroni M, Migliavacca M, Manca G, Cogliati S, Busetto L, Picchi V, Cescatti A, Seufert G, Colombo R. 2010. High resolution field spectroscopy measurements for estimating gross ecosystem production in a rice field. *Agriculture and Forest Meteorology* **150**:1283–1296 DOI 10.1016/j.agrformet.2010.05.011.

Rossini M, MIgliavacca M, Galvagno M, Meroni M, Cogliati S, Cremonese E, Fava R, Gitelson A, Julitta T, Morra di Cella U, Siniscalo C, Colombo R. 2014. Remote estimation of grassland gross primary production during extreme meteorological seasons. *International Journal of Applied Earth Observation and Geoinformation* **29(1)**:1–10 DOI 10.1016/j.jag.2013.12.008.

Roujean JL, Breon FM. 1995. Estimating PAR absorbed by vegetation from bi-directional reflectance measurements. *Remote Sensing of Environment* **51**:375–384 DOI 10.1016/0034-4257(94)00114-3.

Rouse JW, Haas RH, Schell JA, Deering DW. 1973. Monitoring the vernal advancement and retrogradation (green wave effect) of natural vegetation. Progress Report RSC 1978-1, Remote Sensing Center. Texas A & M Univ., College Station, 93 (NTIS No. E73-106393.

Ruimy A, Saugier B, Dedieu G. 1994. Methodology for the estimation of terrestrial net primary production from remotely sensed data. *Journal of Geophysical Research* **99(D3)**:5263–5283 DOI 10.1029/93JD03221.

Running SR, Nemani RR, Heinsch F, Zhao M, Reeves M, Hashimoto H. 2004. A continuous satellite-derived measure of global terrestrial primary production. *Bioscience* **54(6)**:547–560 DOI 10.1641/0006-3568(2004)054[0547:ACSMOG]2.0.CO;2.

Sakowska K, Juszczak R, Gianelle D. 2016. Remote sensing of grassland biophysical parameters in the context of the Sentinel 2 satellite mission. *Journal of Sensors* **2016**:4612809 DOI 10.1155/2016/4612809.

Sakowska K, Vescovo L, Marcolla B, Juszczak R, Olejnik J, Gianelle D. 2014. Monitoring of carbon dioxide fluxes in a subalpine grassland ecosystem of the Italian Alps using a multispectral sensor. *Biogeosciences* **11**:4695–4712 DOI 10.5194/bg-11-4695-2014.

Sims DA, Luo H, Hastings S, Oechel WC, Rahman AF, Gamon JA. 2006. Parallel adjustments in vegetation greenness and ecosystem CO_2 exchange in response to drought in a Southern California chaparral ecosystem. *Remote Sensing of Environment* **103**:289–303 DOI 10.1016/j.rse.2005.01.020.

Sjöström M, Ardö J, Eklundh L, El-Tahir BA, El-Khidir HAM, Hellström M, Pilesjö P, Seaquist J. 2009. Evaluation of satellite based indices for gross primary production estimates in a sparse savanna in the Sudan. *Biogeosciences* **6**:129–138 DOI 10.5194/bg-6-129-2009.

Skinner RH, Wylie BK, Gilmanov TG. 2011. Using normalized difference vegetation index to estimate carbon fluxes from small rotationally grazed pastures. *Agronomy Journal* **103**:972–979 DOI 10.2134/agronj2010.0495.

Spanner M, Pierce LL, Peterson DL, Running SW. 1990. Remote sensing of temperate coniferous forest leaf area index. The influence of canopy closure, understory vegetation and background reflectance. *International Journal of Remote Sensing* **1**:95–111.

Urbaniak M, Chojnicki B, Juszczak R, Augustin J, Leśny J, Ziemblińska K, Sakowska K, Siedlecki P, Olejnik J. 2016. Measuring major components of the carbon balance. In: Mueller L, Sheudshen AK, Eulenstein F, eds. *Novel methods for monitoring and managing land and water resources in siberia*. Cham: Springer Water, 2016 DOI 10.1007/978-3-319-24409-9.

Uździcka B, Strózecki M, Urbaniak M, Juszczak R. 2017. Dependence of spectral characteristics on parameters describing CO_2 exchange between crop species and the atmosphere. *International Agrophysics* **31**:419–432 DOI 10.1515/intag-2016-0059.

Veroustraete F, Patyn J, Myneni RB. 1996. Estimating net ecosystem exchange of carbon using the normalized difference vegetation index and an ecosystem model. *Remote Sensing of Environment* **58**:115–130 DOI 10.1016/0034-4257(95)00258-8.

Verrelst J, Camps-Valls G, Muñoz Marí J, Rivera JP, Veroustraete F, Clevers JGPW, Moreno J. 2015. Optical remote sensing and the retrieval of terrestrial vegetation bio-geophysical properties—a review. *ISPRS Journal of Photogrammetry and Remote Sensing* **108**:273–290 DOI 10.1016/j.isprsjprs.2015.05.005.

Vescovo L, Wohlfahrt G, Balzarolo M, Pilloni S, Sottocornola M, Rodeghiero M, Gianelle D. 2012. New spectral vegetation indices based on the near-infrared shoulder wavelengths for remote detection of grassland phytomass. *International Journal of Remote Sensing* **33/7**:2178–2195.

Vina A, Gitelson AA. 2005. New developments in the remote estimation of the fraction of absorbed photosynthetically active radiation in crops. *Geophysical Research Letters* **32**:L17403 DOI 10.1029/2005GL023647.

Wang Q, Tenhunen J, Dinh NQ, Reichstein M, Vesala T, Keronen. 2004. Similarities in ground- and satellite-based NDVI time series and their relationship to physiological activity of a Scots pine forest in Finland. *Remote Sensing of Environment* **93**:225–237 DOI 10.1016/j.rse.2004.07.006.

Waring RH, Landsberg JJ, Williams M. 1998. Net primary production of forests: a constant fraction of gross primary production? *Tree Physiology* **18**:129–134 DOI 10.1093/treephys/18.2.129.

Wu C, Niu Z, Tang Q, Huang W, Rivard B, Feng J. 2009. Remote estimation of gross primary production in wheat using chlorophyll-related vegetation indices. *Agriculture and Forest Meteorology* **149**:1015–1021 DOI 10.1016/j.agrformet.2008.12.007.

Xiao X, Zhang Q, Braswell B, Urbanski S, Boles S, Wofsy S, Moore III B, Ojima D. 2004. Modeling gross primary production of temperate deciduous broadleaf forest using satellite images and climate data. *Remote Sensing of Environment* **91**:256–270 DOI 10.1016/j.rse.2004.03.010.

Zarco-Tejada PJ, Ustin SL, Whiting ML. 2005. Temporal and spatial relationships between within-field yield variability in cotton and high spatial hyperspectral remote sensing imagery. *Agronomy Journal* **97**:641–653 DOI 10.2134/agronj2003.0257.

Zheng G, Moskal M. 2009. Retrieving Leaf Area Index (LAI) using remote sensing: theories methods and sensors. *Sensors* **9**:2719–2745 DOI 10.3390/s90402719.